NACA RM E52J09

NACA

# RESEARCH MEMORANDUM

## EFFECT OF LINER AIR-ENTRY HOLES, FUEL STATE, AND COMBUSTOR SIZE ON PERFORMANCE OF AN ANNULAR TURBOJET COMBUSTOR AT LOW PRESSURES AND HIGH AIR-FLOW RATES

By Carl T. Norgren and J. Howard Childs

Lewis Flight Propulsion Laboratory
Cleveland, Ohio

NATIONAL ADVISORY COMMITTEE
FOR AERONAUTICS

WASHINGTON
January 13, 1953
Declassified August 19, 1960

NACA RM E52J09

NATIONAL ADVISORY COMMITTEE FOR AERONAUTICS

RESEARCH MEMORANDUM

# EFFECT OF LINER AIR-ENTRY HOLES, FUEL STATE, AND COMBUSTOR SIZE ON PERFORMANCE OF AN ANNULAR TURBOJET COMBUSTOR AT LOW PRESSURES AND HIGH AIR-FLOW RATES

By Carl T. Norgren and J. Howard Childs

## SUMMARY

As part of a general program to determine design criteria for turbojet combustors, an annular combustor was developed by utilizing the design principles evolved in previous investigations and by making 12 design changes to optimize the altitude performance of the combustor. Although the combustor was developed for liquid fuel injection, heated liquid and vapor fuels gave higher combustion efficiencies at the severe operating conditions. At conditions simulating cruise speed at 80,000 feet in a typical turbojet with a 5.2 pressure ratio engine, the heated liquid and vapor fuels gave combustion efficiencies 18 and 23 percent, respectively, above the efficiency obtained with liquid fuel. With all three fuel types the combustion efficiency was higher at severe operating conditions than the efficiency of any of 14 turbojet combustors previously investigated. At rated engine speed the efficiency was above 97 percent with both liquid and vapor fuels at altitudes up to 65,000 feet. The combustion efficiency was slightly increased by increasing the air-flow rate per unit combustor frontal area to a value 30 percent above that used in current engine design. A further increase in the air-flow rate to a value 69 percent above that of current practice resulted in markedly lower combustion efficiencies at the higher fuel-air ratios.

The combustor operated with high combustion efficiency at conditions where a similar but smaller combustor would not operate in a previous investigation; the better performance of the combustor may therefore be due chiefly to its larger size. Combustion efficiencies obtained in previous investigations with 14 different turbojet combustors at comparable operating conditions show a general trend of increase in efficiency with increase in combustor size.

The total-pressure drop of the combustor was approximately twice as great as the value obtained with some production-model combustors. The combustor-outlet temperature profiles followed the pattern generally

desired in turbojet engines. No investigation was made of the combustor durability, carbon-forming tendencies, or other low-altitude operating problems.

## INTRODUCTION

Trends toward higher flight speeds and higher flight altitudes for military aircraft result in a need for larger (higher thrust) turbojet engines and engines which operate more efficiently at high altitudes. This means that combustor size must be increased and that the combustion efficiency must be increased at the severe, low-pressure conditions encountered with reduced-throttle operation at high altitudes. The attendant improvements in compressor performance may be expected to make possible higher air-flow rates per unit compressor frontal area. If the combustor is not to become the engine component requiring the greatest frontal area, then combustors must be developed which can produce high combustion efficiencies at high air-flow rates per unit combustor frontal area.

Research at the NACA Lewis laboratory on designs for annular turbojet combustors (references 1 to 3) has resulted in improved altitude performance of these combustors. Other NACA research (references 4 and 5) has shown that the use of vapor fuel in lieu of the design (liquid) fuel in a turbojet combustor improved the combustion efficiency at severe operating conditions.

The research reported herein consisted of a direct-connect duct investigation of a one-quarter segment of a $25\frac{1}{2}$-inch-diameter annular turbojet combustor. This research had a fourfold objective: (1) to develop a combustor using design techniques evolved in previous investigations (references 1 to 3) which will provide high combustion efficiency at low-pressure operating conditions; (2) to investigate the performance of this combustor with heated liquid and vapor fuels using the conventional liquid-fuel injection system; (3) to determine the combustion efficiency of this combustor at the high air-flow rates per unit frontal area which may be produced by future improvements in compressor design; and (4) to compare the efficiency of this combustor with similar data obtained in a previous investigation with a similar, but smaller combustor (unpublished data) in order to show the effect of combustor size on efficiency.

An annular combustor configuration was selected for this investigation because this configuration best utilizes the space available for combustion in a turbojet engine. The fuel injection system was made similar to those used in all annular combustors previously investigated at this laboratory, and consisted of hollow-cone-spray pressure atomizers

located at the upstream end of the combustor liner and injecting fuel in the downstream direction. The selection of combustor size and liner design was based on the results of previous investigations in the manner described in the following paragraphs.

Design modifications made with two different annular turbojet combustors by altering the size and arrangement of the circular air-admission holes in the combustor liner resulted in improved combustion efficiencies and altitude operating limits (reference 1 and unpublished data). With both these combustors the best altitude performance was obtained with approximately the same arrangement of circular holes in the upstream portion of the combustor liner. In reference 2 further design modifications were made in order to improve the combustor-outlet temperature profile. Narrow longitudinal slots for admission of air through the upstream portion of the liner were shown to permit better control of the outlet-temperature profile. The combustion efficiencies obtained in reference 2 were about the same as the efficiencies obtained with the optimum arrangement of circular holes in this same combustor (unpublished data), indicating that the longitudinal slots for air admission did not afford any important gains in combustion efficiency. In reference 3 the air-admission slots were utilized in the design of a larger combustor. This slotted annular combustor of reference 3 is listed as combustor G in reference 6, where its combustion efficiency is compared with that of various other turbojet combustors. These performance comparisons show that the slotted annular combustor of reference 3 produces the highest combustion efficiencies at the severe operating conditions of the 14 turbojet combustors of reference 6.

Since the earlier investigations with a smaller combustor had shown that slots for air admission provide no important increase in combustion efficiency over the values attainable with circular holes, it would appear possible to obtain combustion efficiencies comparable with those of the slotted annular combustor of reference 3 through the use of the optimum arrangement of circular holes in a combustor of the same size. Previous investigations (reference 7) had shown that combustor liners having circular holes are far less subject to warping than the liners having narrow longitudinal slots for primary air admission. Consequently, the combustor selected for the investigation reported herein was made identical in size to the slotted annular combustor of reference 3, and the design included an arrangement of circular holes in the upstream portion of the liner which was similar to the optimum hole arrangement evolved in reference 1. Rectangular slots were used in the downstream portion of the liner because previous experience (unpublished data) had shown these to be a suitable means for obtaining the desired combustor-outlet temperature profile.

With this basic combustor configuration, a total of 12 design modifications was made to optimize the performance; that is, to obtain

the best combination of high efficiency, low pressure drop, and desired outlet-temperature profile. The experimental investigation with the final combustor (model 13) included combustion efficiencies, pressure losses, and outlet-temperature profiles. The investigation was conducted with liquid, heated liquid, and vapor fuels and with several fuel atomizers. Low-pressure operating conditions were investigated to simulate high-altitude flight with air-flow rates per unit combustor frontal area which are typical of current engine design practice, 30 percent above current practice, and 69 percent above current practice. The combustion efficiency data for a range of operating conditions were generalized to fall on a common curve, and this correlation was used to predict the combustion efficiency to be expected with the model 13 combustor at various flight conditions in a turbojet engine. Comparisons were made of the performance of the model 13 combustor with similar data obtained in previous investigations with other combustors to show the relative performance of the model 13 combustor and to indicate the effect of combustor size on performance.

## APPARATUS

### Installation

A diagram of the combustor installation is shown in figure 1. The combustor-inlet and combustor-outlet ducts were connected to the laboratory air supply and low-pressure exhaust systems, respectively. Air-flow rates and combustor pressures were regulated by remote-controlled valves upstream and downstream of the combustor. The combustor-inlet air temperature was controlled by an electric air heater. Fuel preheat was supplied by an electric resistance-type heater.

### Instrumentation

Air flow was metered by a concentric-hole, sharp-edge orifice installed according to A.S.M.E. specifications. Liquid fuel flow was metered by a calibrated rotameter; vapor fuel flow, by a calibrated sharp-edge orifice. Thermocouples and pressure tubes were located at the combustor inlet and outlet planes as indicated in figure 1. The number, type, and location of these instruments at each plane is indicated in figure 2. The combustor-outlet thermocouples were located at centers of equal areas in the duct. Details of construction of the thermocouples and pressure tubes are shown in figure 3 and are the same as those presented in reference 3. Pressure tubes were connected to absolute manometers; thermocouples were connected to a recording potentiometer.

## Combustors

A total of 13 combustor configurations was investigated. Each combustor consisted of a one-quarter segment (90°) of a single-annulus combustor having an outside diameter of $25\frac{1}{2}$ inches, an inside diameter of $10\frac{5}{8}$ inches, and a length from fuel atomizers to combustor-outlet thermocouples of approximately 23 inches. The maximum combustor cross-sectional area was 105 square inches (corresponding to 420 square inches for the complete combustor). Ten simplex hollow-cone-spray pressure atomizers (corresponding to 40 atomizers in the complete combustor) injected the fuel in the downstream direction from the upstream end of the combustor liner. Several sets of atomizers of different capacity were used in the course of the experimental investigation.

Figure 4 shows a three-quarter cut-away view of the final combustor (model 13) and figure 5, a longitudinal cross section of the combustor. The arrangement of air-admission holes in the liner of model 13 combustor is shown in figure 6. In the present discussion the upstream one-half of the liner will be referred to as the primary zone and the second one-half, as the secondary zone.

## Fuels

The liquid fuel used in this investigation was MIL-F-5624A grade JP-4. The inspection data for this fuel are presented in table I. The vapor fuel was commercial propane.

## PROCEDURE

Combustion efficiency and combustor total-pressure loss data were recorded for a range of fuel-air ratio at the following conditions:

| Condition | Combustor-inlet total pressure (in. Hg absolute) | Combustor-inlet total temperature (°F) | Air-flow rate per unit combustor area[a] (lb/(sec)(sq ft)) | Simulated flight altitude in reference engine at cruise rpm (ft) |
|---|---|---|---|---|
| A | 15 | 268 | 2.14 | 56,000 |
| B | 8 | 268 | 1.14 | 70,000 |
| C | 5 | 268 | 0.714 | 80,000 |
| D | 15 | 268 | 2.78 | 56,000 |
| E | 15 | 268 | 3.62 | 56,000 |

[a]Based on maximum combustor cross-sectional area.

These conditions simulate operation of the combustor in a reference turbojet engine, which is a typical 5.2 pressure ratio turbojet, operating at a Mach number of 0.6. The cruise speed of the engine is assumed to be 85 percent of the rated rotor speed. Test conditions A through C require air-flow rates per unit combustor frontal area which are typical of current turbojet engines. Test conditions D and E require air-flow rates which are 30 percent and 69 percent, respectively, above current practice.

In the preliminary research necessary to evolve the final combustor design, limited data were recorded with JP-4 fuel and 10.5-gallon-per-hour atomizers in each combustor at one or more of test conditions A, B, and C. With the final (model 13) combustor, more extensive data were recorded, as indicated in the following table:

| Fuel | Fuel atomizer capacity (gal/hr)[a] | Fuel spray angle (deg)[a] | Conditions |
|---|---|---|---|
| JP-4 | 10.5 | 60 | A,B,C,D,E |
| | 3.0 | 60 | A,B,C |
| Heated JP-4[b] | 10.5 | 60 | A,B,C |
| Propane | 10.5 | 60 | B,C |
| | 30 | 70 | A,B,C,D,E |
| | 60 | 70 | E |

[a]Rated at 100 lb/sq in. pressure differential; liquid fuel.

[b]Fuel temperature, 300° F.

Combustion efficiency was computed as the percentage ratio of actual to theoretical increase in enthalpy from the combustor-inlet to the combustor-outlet instrumentation planes using the method of reference 8. For calculation of combustor-outlet enthalpy, the temperature was computed as the arithmetic mean of the 30 outlet thermocouple indications; no corrections were made for radiation or velocity effects on the thermocouple indications.

Combustor reference velocities were computed from the air mass-flow rate, the combustor-inlet density, and the maximum combustor cross-sectional area (105 sq in.). The total-pressure loss was computed as the dimensionless ratio of the total-pressure loss to the combustor reference dynamic pressure using the method of reference 3. The radial

distribution of temperatures at the combustor outlet was determined at each test condition investigated and at two values of combustor temperature rise (approximately 680° and 1180° F, the required values at 85 and 100 percent rated speed in the reference turbojet engine at altitudes above the tropopause). The temperature at each of the 5 radial positions was computed as the average of four thermocouple readings at each radial position (see fig. 2(b)). The temperature rake at each side wall of the combustor was not included in these average temperatures in order to minimize the effects of the side walls on temperature readings. The optimum combustor-outlet radial temperature profile was considered to be that shown in figure 7; this temperature profile represents an approximate average of those profiles required or desired in various turbojet engines.

## RESULTS

The results obtained in the investigation of the preliminary combustor configurations are discussed briefly in appendix A. The following results were obtained with the final (model 13) combustor. The model 13 combustor was considered to be a near-optimum design for the particular combustor size and shape, fuel, and fuel injection system which were selected and for the particular test conditions investigated; it gave the best over-all performance of the 13 combustor configurations investigated. The experimental data for the model 13 combustor are presented in table II. A tabulated list of all symbols is presented in appendix B.

### Combustion Efficiencies

The combustion efficiencies obtained with liquid, heated liquid, and vapor fuels are presented in figures 8, 9, and 10, respectively, for a range of fuel-air ratio at each of three inlet pressures (test conditions A, B, and C). The data of figures 8 and 9 were obtained with 10.5-gallon-per-hour, 60° fuel atomizers. These same atomizers were used with vapor fuel to obtain a part of the data of figure 10. Additional data are shown in figure 10 for 30-gallon-per-hour, 70° atomizers.

Duplicate data were recorded at a few values of fuel-air ratio at test conditions B and C, and these check data are indicated by tailed symbols in figure 8. The check data showed an average deviation of $\pm 2$ percent.

Figure 11 presents combustion efficiencies at the same test conditions as the preceding figures (test conditions A, B, and C) with liquid fuel and improved fuel atomization through the use of 3.0-gallon-per-hour, 60° atomizers.

Figures 12 and 13 show combustion efficiencies obtained at three air-flow rates (test conditions A, D, and E) with liquid and vapor fuels, respectively. The data of figure 12 were obtained with 10.5-gallon-per-hour, 60° fuel atomizers. The data of figure 13 for vapor fuel were obtained with two atomizer capacities, 30-gallon-per-hour and 60-gallon-per-hour atomizers. The 60-gallon-per-hour atomizers were required to obtain the higher fuel-air ratios at test condition E without causing the pressure drop in the fuel injectors to exceed the propane fuel supply pressure, which was approximately 80 pounds per square inch gage.

### Pressure Losses

The pressure losses through the combustor are presented in figure 14. The dimensionless ratio of the total-pressure drop to the reference dynamic pressure $\Delta P/q_r$ is plotted as a function of the combustor-inlet to combustor-outlet density ratio $\rho_1/\rho_2$. The expected straight-line relation is obtained, but some separation occurs between data recorded at different pressures.

### Outlet Temperature Profiles

Figures 15(a) and 15(b) show combustor-outlet radial temperature profiles with liquid and vapor fuels, respectively, at each condition investigated and at two values of combustor temperature rise (approximately 680° and 1180° F). The desired temperature profile from figure 7 is included for comparison.

## DISCUSSION

### Fuel State

A comparison of the curves from figures 8 to 10 is presented in figure 16 to show the effect of fuel state on combustion efficiency. Only slight differences exist among the liquid, heated liquid, and vapor fuels at the two higher pressures (conditions A and B). At the most severe test condition investigated, corresponding to cruise speed at 80,000 feet altitude (condition C), the combustion efficiency with the vapor fuel was 23 percent above that with liquid fuel and the efficiency with heated liquid fuel was 18 percent above that with liquid fuel; these comparisons are made at the fuel-air ratios required with each fuel to give the 680° F combustor temperature rise required for cruise speed in the reference engine at 80,000 feet altitude. These values of fuel-air ratio are indicated by circular symbols on each of the curves for test condition C in figure 16.

The curves for liquid and vapor fuel at the highest air-flow rate (condition E, figs. 12 and 13) show that vapor fuel also provides a significant increase in combustion efficiency at this severe operating condition. The higher combustion efficiency of the vapor fuel at severe operating conditions is in accord with the results of previous investigations of liquid and vapor fuels in turbojet combustors (references 4 and 5).

A comparison of the data of figure 11 with the data of figure 8 shows that the smaller capacity atomizers gave no significant increase in efficiency at any of the conditions investigated, and that they caused a slight decrease in efficiency at the lowest pressure (condition C). Thus the higher combustion efficiencies obtained with heated liquid and vapor fuels were not obtained by finer mechanical atomization of the liquid fuel.

## Performance Comparisons

Most turbojet combustor investigations have been conducted at test conditions simulating operation of each combustor in its particular engine; consequently, it is difficult to find data obtained with different combustors at identical operating conditions. The combustion parameter $V_r/p_i\ T_i$ (where $V_r$ is the combustor reference velocity in ft/sec, calculated from inlet density, mass-flow rate, and maximum combustor cross-sectional area; $p_i$ is the combustor-inlet static pressure in lb/sq ft absolute; and $T_i$ is the combustor-inlet temperature in $^{\circ}R$) can be used, however, to reduce the combustion efficiencies obtained at any test conditions to a single curve for each combustor and each fuel, as shown in reference 6. A comparison of these curves therefore affords a comparison of the performance of various combustors even though the experimental conditions investigated might be different for the various combustors.

In figure 17 are plotted the combustion efficiency data of figures 8, 9, 10, 12, and 13 as a function of the combustion parameter $V_r/p_i\ T_i$. This form of the parameter is used herein rather than its reciprocal $p_i\ T_i/V_r$ as derived in reference 6 because the resulting correlation curves do not have the extreme curvature noted in reference 6. The efficiency data of figure 17(a) are for a combustor temperature rise of 680° F, which is the value required in the reference engine at cruise speed and altitudes above the tropopause. Figures 17(b) and 17(c) present similar data for values of temperature rise of 402° and 1180° F, which are the required values of temperature rise for 75- and 100-percent rated speed at altitudes above the tropopause. These values of required temperature rise were obtained from

engine performance curves which were extrapolated to the higher altitude conditions by assuming constant efficiencies of engine components other than the combustor. Figure 18 presents a comparison of the curves of figure 17 for the model 13 combustor with liquid, heated liquid, and vapor fuels with similar curves for two of the better combustors (combustors G and L) reported in reference 6. Combustor G from reference 6 is the slotted annular combustor of reference 3, which produced the highest combustion efficiencies of the 14 turbojet combustors reported in reference 6. Combustor L from reference 6 is one of the better production-model combustors. Figure 18 shows that with any of the three fuel types investigated, the model 13 combustor produced a higher combustion efficiency at severe operating conditions than any of the 14 combustors of reference 6.

## Estimated Flight Performance

Figure 19(a) shows the estimated combustion efficiency of the model 13 combustor with liquid fuel at various flight conditions in the reference turbojet engine. The curves of constant combustion efficiency were obtained as follows: At each flight condition indicated on figure 19(a) by a circular symbol, the required temperature rise and the value of the combustion parameter $V_r/p_i T_i$ were obtained from the engine performance curves. For each value of the combustion parameter thus obtained the corresponding efficiency was then obtained from figure 17 for values of temperature rise above and below the required value. The efficiency at the required temperature rise was then obtained by interpolation. These values of combustion efficiency were next indicated in figure 19(a) beside the appropriate circular symbols. Finally, the constant efficiency curves were drawn to fit the pattern indicated by these circular symbols.

The three rectangular data points in figure 19(a) at 85 percent rated speed represent actual experimental data where the test conditions accurately simulated flight operation at the conditions indicated on the figure. The combustion efficiencies listed beside each of these three data points match well with the values expected from interpolation between the curves, indicating the validity of figure 19(a). The curves of figure 19(a) show that with liquid fuel the model 13 combustor operated at efficiencies above 97 percent up to an altitude of 65,000 feet at rated engine speed.

Similar data are presented in figure 19(b) for the model 13 combustor operating with vapor fuel. Again the circular symbols represent data calculated by use of figure 17, and the square symbols represent experimental data. With vapor fuel the model 13 combustor operated at efficiencies above 97 percent up to an altitude of 65,000 feet at rated engine speed.

With both liquid and vapor fuel the model 13 combustor supplied sufficient temperature rise to operate the turbojet engine at 85 percent rated speed and an altitude of 80,000 feet. Thus the altitude operating limits of the engine would lie above 80,000 feet at 85 percent rated speed.

## High Air-Flow Rates

The combustion efficiency of the model 13 combustor was slightly increased with both liquid and vapor fuels when the air-flow rate per unit frontal area was increased to a value about 30 percent above current design practice (figs. 12 and 13). This result is contrary to the usual trend of decreased efficiency with increased velocity which has been generally noted in previous investigations. When this air flow was further increased to a value about 69 percent above current practice, the efficiency with both fuels was markedly decreased at high fuel-air ratios. The vapor fuel gave higher efficiencies than the liquid fuel at the highest air-flow rate, indicating that a combustor designed to make better use of the vapor fuel might constitute one means for obtaining high efficiencies at higher air-flow rates.

## Combustor Size

A development program similar to that reported herein was previously conducted with an annular combustor of smaller size (unpublished data). The model 13 combustor evolved herein and the smaller combustor previously investigated are similar in many respects: (1) both combustors are annular combustors with similar fuel injection systems; (2) both combustors have approximately the same arrangement of circular holes in the upstream end of the combustor liner; and (3) both combustors produced higher efficiencies than the various other combustor configurations which were investigated in their respective development programs. These combustors differ primarily in size. A comparison of the performance of these two combustors should therefore provide some indication of the effect of combustor size on performance.

A significant comparison of the combustion efficiency of these two combustors is not available because the combustion efficiencies of the smaller combustor were measured only at favorable conditions corresponding to low values of the combustion parameter $V_r/p_i\ T_i$ where most combustors give efficiencies near 100 percent. The best available performance comparison between these two combustors is therefore shown in figure 20. The altitude operating limits of the smaller combustor appear as a straight line. The experimental data obtained with the model 13 combustor are also included in figure 20 to show that the model 13 combustor operated with high efficiency over a wide range of conditions where the smaller combustor would not operate.

The indicated effect of combustor size may possibly be the result of liquid fuel "wash" on the walls of the combustor liner. Reference 9 shows air- and fuel-flow patterns in a turbojet combustor with no burning occurring, and an appreciable quantity of the liquid fuel impinges on the walls of the liner and flows along the walls as a continuous liquid film. Liquid fuel "wash" along the walls of the liner has also been observed under burning conditions in some combustors. Large quantities of liquid fuel on the walls would be expected to result in a decrease in combustion efficiency. Since the fuel atomizers used in the smaller combustor had the same flow capacity and spray angle as those used in the model 13 combustor, it would be expected that they would cause much greater quantities of liquid fuel to impinge on the walls of the smaller combustor.

Further indication of a possible important effect of combustor size on combustion efficiency is shown in figure 21. Values of combustion efficiency obtained in previous investigations with 14 different turbojet combustors at operating conditions of equal severity ($V_r/p_i\ T_i = 100 \times 10^{-6}$) are plotted in figure 21 as a function of a combustor hydraulic radius. The efficiency data for these fourteen combustors were taken from the curves of reference 6. The combustor hydraulic radius is defined as the ratio of the cross-sectional area inside the combustor liner to the wetted perimeter of the combustion zone at the point where the undisturbed fuel spray would touch the liner walls. This hydraulic radius is also the volume-to-surface ratio per unit length of the combustion zone at the point where the fuel is dispersed across the combustion zone. A combustor hydraulic radius was selected as an index of the effect of combustor size on efficiency because the surface-to-volume ratio of small-scale combustion apparatus is known to have an important effect on flammability limits, as shown in reference 10. The point where the undisturbed fuel spray would touch the liner walls was arbitrarily selected as the plane at which the hydraulic radius would be evaluated; a better correlation of the data of figure 21 might possibly be obtained by using values of hydraulic radius which are evaluated differently.

Figure 21 shows that the data points for most of the 14 combustors of reference 6 fall within $\pm 10$ percent of a single curve, and this curve shows an increase in combustion efficiency with increase in combustor size throughout the range of size investigated. The data point for the model 13 combustor falls near the upper end of the curve in figure 21. Other design factors besides that of size are, of course, important, and this accounts for some of the scatter of data points in figure 21. For example, combustors C and D are identical except for changes in the primary air holes in the liner, and combustors I and J are identical except for changes in the fuel atomizer.

### Pressure Losses, Outlet Temperature Profiles, and Other Performance Characteristics

For isothermal (no combustion) flow, the average value of $\Delta P/q_r$ in figure 14 is about 25; this value is approximately twice as great as the corresponding value for some production-model combustors. The design changes which were made in an attempt to reduce this pressure drop were unsuccessful, as noted in appendix A; with a more extensive effort it might, however, be possible to significantly reduce this pressure drop.

The combustor-outlet temperature profiles in figure 15 are similar to the profile generally desired in turbojet engines, with low temperatures near the blade hub and blade tip positions and a maximum temperature at about 85 percent of the blade height. The maximum circumferential scatter of individual thermocouple indications was $\pm 200^{\circ}$ F at any radial position. The outlet-temperature profiles for the model 13 combustor were not so good as those of some of the preliminary combustors investigated (for example, see appendix A) because the model 13 combustor was evolved as the result of design compromises to obtain the best over-all combination of high efficiency, low pressure drop, and a desired pattern of outlet temperatures.

The low altitude performance of the combustor was not investigated; consequently, little is known regarding its durability or carbon-deposition characteristics. No carbon deposits or warping of the liner were observed during this investigation, but the test conditions were not in the range where these problems are severe.

## SUMMARY OF RESULTS

An annular turbojet combustor was developed to give improved performance at high altitudes by utilizing the design principles evolved in previous investigations to obtain the basic combustor configuration and then making 12 minor design changes to optimize the performance of this combustor. The results obtained from the experimental investigation of the model 13 combustor at low pressures and high air-flow rates are summarized in the following paragraphs. The values quoted for simulated flight performance refer to the model 13 combustor in a typical 5.2 pressure ratio turbojet engine at a flight Mach number of 0.6.

1. Although the combustor was developed for liquid fuel injection, heated liquid and vapor fuels injected through the conventional liquid-fuel injection system gave higher combustion efficiencies at the more severe operating conditions. At conditions simulating cruise speed at

80,000 feet altitude, the efficiencies with heated liquid and vapor fuels were 18 and 23 percent, respectively, above the efficiency with liquid fuel. At cruise speed at 70,000 feet, the differences in efficiency between the fuels were slight.

2. With all three fuel types investigated (liquid, heated liquid, and vapor) the combustion efficiency at severe operating conditions was higher than the efficiency of any of 14 turbojet combustors previously investigated. At rated engine speed the combustion efficiency was above 97 percent with both liquid fuel and vapor fuel at altitudes up to 65,000 feet.

3. At cruise speed at 56,000 feet altitude, the combustion efficiency was slightly increased by increasing the air-flow rate per unit combustor frontal area to a value 30 percent above that used in current engine design practice. At an air-flow rate 69 percent above current practice, however, the efficiency was markedly decreased at high fuel-air ratios.

4. A smaller, similar annular combustor which was previously developed to obtain high performance would not operate at many conditions at which the model 13 combustor produced high efficiency. The better performance of the model 13 combustor may therefore be due chiefly to its size. A comparison of the combustion efficiency previously obtained with 14 turbojet combustors at comparable operating conditions shows that for most of the combustors the efficiency increases with increase in combustor size.

5. The total-pressure drop through the combustor was approximately twice as great as the pressure drop of some production-model combustors.

6. The combustor-outlet temperatures followed the radial pattern generally desired in turbojet engines; that is, the temperatures were low at the extreme blade hub and blade tip positions and were a maximum at about 85 percent of the blade height. The maximum circumferential variation of individual thermocouple indications from the mean temperature at any radial position was about $\pm 200^{\circ}$ F.

7. The low-altitude performance of the combustor has not been investigated; consequently, little is known regarding its durability or carbon-deposition characteristics.

Lewis Flight Propulsion Laboratory
National Advisory Committee for Aeronautics
Cleveland, Ohio

# APPENDIX A

## EVOLUTION OF MODEL 13 COMBUSTOR

The design modifications consisted of two distinct types: (1) secondary zone modifications, which primarily affected the outlet-temperature profile and the combustor pressure drop; and (2) primary zone modifications, which primarily affected the combustion efficiency. The greatest deficiency of the model 1 combustor was its outlet-temperature profile; hence secondary zone modifications were made first.

### Secondary Zone Modifications

Figure 22 shows the combustor liner design for three combustors (models 1, 2, and 3), and figure 23 shows the radial outlet-temperature profiles of these combustors. Combustor models 1 to 3 had approximately the same total open area in the liner and hence the same pressure drop. Model 1 produced temperatures which were too low near the inner wall (turbine blade hub) and too high near the center of the duct (fig. 23(a)).

Model 2 was evolved to improve the temperature profile of model 1. This combustor had less open area on the inner wall of the liner and correspondingly greater open area on the outer wall, resulting in increased temperatures near the blade hub (fig. 23(b)). In addition, the model 2 combustor had a greater spacing between the air-admission slots in the inner wall of the liner, permitting the cold air entering through these slots to penetrate as individual jets into the hot gases to produce alternate hot and cold "corridors" in the combustor. With the smaller slot spacing of the preceding combustor (model 1), these air jets did not penetrate as individual jets, but displaced the hot gases toward the center of the duct and coalesced to form a cold layer of gas near the turbine blade hub. These deductions are based on observations of the flame patterns in the combustor and the temperature patterns visible on the side walls of the combustor housing. The improved jet penetration (obtained with the model 2 combustor) served to reduce the temperature in the center of the duct (fig. 23(b)).

The model 3 combustor represented a still further step in the same direction; that is, less open area in the inner wall, correspondingly greater open area in the outer wall, and wider spacing between the slots in the inner wall. A further improvement in outlet-temperature profile resulted (fig. 23(c)).

An increase in the area of the secondary zone liner perforations was required to decrease the pressure drop of the model 3 combustor. The width of the secondary zone slots could not be increased without

reducing the space between the secondary air jets; this would be expected to impair the penetration of these jets as indicated by the experience with combustor models 1 to 3. The slots could not be extended upstream without reducing the length available for combustion. The requisite increase in area of the slots was therefore obtained by changing from 10 slots (fig. 22) to 5 slots (fig. 6); this permitted a 30 percent increase in the area of the secondary air slots in model 13 over that of models 1 to 3. The outlet-temperature profile was slightly impaired by this area increase, but the accompanying decrease (approximately 25 percent) in pressure drop made the over-all performance of the model 13 combustor more desirable.

After the change was made from the 10-slot to the 5-slot secondary zone configuration, three modifications were required to obtain the desired outlet-temperature profile by means of a correct balance between secondary slot area in the outer wall and in the inner wall of the liner (models 11 to 13).

Attempts to greatly increase the area of the secondary air slots (models 5 and 6) resulted in circumferentially uneven temperature profiles and severe local high-temperature regions. Models 5 and 6 also showed no marked lowering of the pressure drop, probably because a large part of the pressure loss was then occurring in the annular flow passages which supply air to the downstream part of the combustor liner.

Additional secondary zone modifications were made in models 7 and 8 to add cooling louvers at the positions indicated in figure 6.

### Primary Zone Modifications

Combustor model 4 was similar to model 3 but had 3 rows of holes consisting of ten 3/16-inch holes per row located in the inner and outer walls of the liner (for a total of sixty 3/16-inch holes in the one-quarter sector) approximately $7\frac{1}{2}$ inches from the upstream end of the liner. These small holes had no measurable effect on performance and were later replaced by a row of cooling louvers.

Combustor models 9 and 10 varied the amount of air admitted behind the fuel atomizer radiation shield (fig. 5). This air flows around the fuel atomizers and emerges into the combustion zone through the holes provided in the radiation shield for each fuel atomizer. Model 9 had a row of 1/16-inch holes in the upstream end of the liner walls for admission of this air behind the fuel atomizers; the final model 13 combustor had 1/8-inch diameter holes for this purpose, and the model 10 combustor had alternate 1/8-inch and 5/32-inch holes for this purpose. Thus models 9 and 10 provided less and more air, respectively, around the

fuel atomizers than did model 13. The combustion efficiencies of models 9 and 10 were below that of model 13, indicating that the air admitted around the fuel nozzles has a marked effect on efficiency and further indicating that model 13 provided approximately the optimum quantity of air in this location.

## APPENDIX B

## SYMBOLS

The following symbols are used in this report:

| | |
|---|---|
| $A_r$ | reference combustor cross-sectional area, sq ft |
| $f$ | fuel-air ratio, lb/lb |
| $P_i$ | combustor-inlet total pressure, in. Hg absolute |
| $\Delta P$ | total-pressure drop through combustor, in. Hg |
| $\Delta P_f$ | fuel manifold pressure (above combustor-inlet pressure), in. Hg |
| $p_i$ | combustor-inlet static pressure, lb/sq ft absolute |
| $q_r$ | reference dynamic pressure, in. Hg |
| $T_i$ | combustor-inlet total temperature, $^{o}R$ |
| $T_o$ | mean combustor-outlet temperature, $^{o}R$ |
| $\Delta T$ | mean temperature rise through combustor, $^{o}F$ |
| $V_r$ | combustor reference velocity, ft/sec |
| $W_a$ | air-flow rate, lb/sec |
| $W_f$ | fuel-flow rate, lb/hr |
| $\eta_b$ | combustion efficiency, percent |
| $\rho_1$ | combustor-inlet air density, lb/cu ft |
| $\rho_2$ | combustor-outlet air density, lb/cu ft |

## REFERENCES

1. Olson, Walter T., and Schroeter, Thomas T.: Effect of Distribution of Basket-Hole Area on Simulated Altitude Performance of $25\frac{1}{2}$-Inch-Diameter Annular-Type Turbojet Combustor. NACA RM E8A02, 1948.

2. Mark, Herman, and Zettle, Eugene V.: Effect of Air Distribution on Radial Temperature Distribution in One-Sixth Sector of Annular Turbojet Combustor. NACA RM E9I22, 1950.

3. Zettle, Eugene V., and Mark, Herman: Simulated Altitude Performance of Two Annular Combustors with Continuous Axial Openings for Admission of Primary Air. NACA RM E50E18a, 1950.

4. McCafferty, Richard J.: Vapor-Fuel-Distribution Effects on Combustor Performance of a Single Tubular Combustor. NACA RM E50J03, 1950.

5. McCafferty, Richard J.: Liquid-Fuel-Distribution and Fuel-State Effects on Combustion Performance of a Single Tubular Combustor. NACA RM E51B21, 1951.

6. Childs, J. Howard: Preliminary Correlation of Efficiency of Aircraft Gas-Turbine Combustors for Different Operating Conditions. NACA RM E50F15, 1950.

7. Harp, James L., Jr., and Vincent, Kenneth R.: Altitude Performance Investigation of Single- and Double-Annular Turbojet-Engine Combustors with Various Size Fuel Nozzles. NACA RM E51L14, 1952.

8. Turner, L. Richard, and Bogart, Donald: Constant-Pressure Combustion Charts Including Effects of Diluent Addition. NACA Rep. 937, 1949. (Supersedes NACA TN's 1086 and 1655.)

9. Straight, David M., and Gernon, J. Dean: Photographic Studies of Preignition Environment and Flame Initiation in Turbojet-Engine Combustors. NACA RM E52I11.

10. Belles, Frank E., and Simon, Dorothy M.: Variation of the Pressure Limits of Flame Propagation with Tube Diameter for Propane-Air Mixtures. NACA RM E51J09, 1951.

TABLE I - FUEL ANALYSIS

| Fuel properties | MIL-F-5624A (JP-4) (NACA fuel 52-53) |
|---|---|
| A.S.T.M. distillation D86-46, °F | |
| Initial boiling point | 136 |
| Percentage evaporated | |
| 5 | 183 |
| 10 | 200 |
| 20 | 225 |
| 30 | 244 |
| 40 | 263 |
| 50 | 278 |
| 60 | 301 |
| 70 | 321 |
| 80 | 347 |
| 90 | 400 |
| Final boiling point | 498 |
| Residue, percent | 1.2 |
| Loss, percent | 0.7 |
| Aromatics | |
| A.S.T.M. D-875-46T, percent by volume | 8.5 |
| Silica gel, percent by volume | 10.7 |
| Specific gravity | 0.757 |
| Viscosity, centistokes at 100° F | 0.762 |
| Reid vapor pressure, lb/sq in. | 2.9 |
| Hydrogen-carbon ratio | 0.170 |
| Net heat of combustion | 18,700 |

TABLE II - DATA OBTAINED FOR MODEL 13 COMBUSTOR

| Run | Combustor-inlet total pressure $P_1$ (in. Hg) | Combustor-inlet total temperature $T_1$ ($^\circ$R) | Air flow rate $W_a$ (lb/sec) | Air flow rate per unit area $W_a/A_r$ $\left(\frac{lb}{(sec)(sq\ ft)}\right)$ | Combustor reference velocity $V_r$ (ft/sec) | Fuel flow rate $W_f$ (lb/hr) | Fuel manifold pressure (above combustor-inlet pressure) $\Delta P_f$ (lb/sq in.) | Fuel-air ratio f | Mean combustor-outlet temperature $T_0$ ($^\circ$R) | Mean temperature rise through combustor $\Delta T$ ($^\circ$F) | Combustion efficiency $\eta_b$ (percent) | Total pressure drop through combustor $\Delta P$ (in. Hg) | Combustion parameter $V_r/p_1T_1$ (ft, lb, sec, $^\circ$R units) |
|---|---|---|---|---|---|---|---|---|---|---|---|---|---|
| 10.5 gal/hr, 60° fuel atomizer; fuel, JP-4 | | | | | | | | | | | | | |
| 1 | 15.0 | 728 | 1.560 | 2.137 | 80.46 | ---- | --- | -------- | ---- | ---- | ----- | 0.914 | $100.7\times10^{-6}$ |
| 2 | | 730 | 1.557 | 2.133 | 80.51 | 39.5 | 4.0 | 0.007047 | 1248 | 518 | 99.92 | 1.307 | 100.5 |
| 3 | | 731 | 1.558 | 2.134 | 80.71 | 46.4 | 4.3 | .008272 | 1322 | 591 | 97.87 | 1.358 | 100.6 |
| 4 | | 730 | 1.558 | 2.134 | 80.56 | 53.9 | 4.5 | .009610 | 1403 | 673 | 96.72 | 1.387 | 100.6 |
| 5 | | 720 | 1.562 | 2.140 | 79.65 | 65.0 | 4.7 | .01156 | 1522 | 802 | 96.90 | 1.424 | 100.9 |
| 6 | | 730 | 1.553 | 2.127 | 80.31 | 73.6 | 5.0 | .01316 | 1651 | 921 | 98.98 | 1.475 | 100.2 |
| 7 | | 734 | 1.554 | 2.129 | 80.77 | 85.9 | 5.1 | .01536 | 1773 | 1039 | 96.97 | 1.532 | 100.3 |
| 8 | | 736 | 1.567 | 2.147 | 81.68 | 101.7 | 5.5 | .01803 | 1927 | 1191 | 96.17 | 1.616 | 101.2 |
| 9 | 8.0 | 728 | .8319 | 1.140 | 80.51 | 20.5 | 2.8 | .006845 | 1197 | 469 | 92.82 | .7120 | 188.9 |
| 10 | 7.95 | 722 | .8250 | 1.130 | 79.70 | 25.8 | 2.8 | .008687 | 1249 | 527 | 82.82 | .7408 | 189.6 |
| 11 | 8.0 | 726 | .8319 | 1.140 | 80.31 | 29.3 | 3.0 | .009783 | 1351 | 625 | 88.01 | .7753 | 188.9 |
| 12 | | 723 | .8311 | 1.138 | 79.90 | 40.3 | 3.5 | .01347 | 1496 | 773 | 80.48 | .7954 | 188.6 |
| 13 | | 725 | .8272 | 1.133 | 79.75 | 55.0 | 3.9 | .01847 | 1753 | 1028 | 80.29 | .8404 | 187.7 |
| 14 | | 725 | .8292 | 1.136 | 79.95 | 83.5 | 4.0 | .02797 | 2025 | 1300 | 69.78 | .8877 | 188.2 |
| 15 | 5.0 | 729 | .5192 | .7112 | 80.51 | 21.2 | 3.3 | .01134 | 1244 | 515 | 62.50 | .5002 | 301.7 |
| 16 | | 729 | .5187 | .7105 | 80.46 | 28.0 | 4.1 | .01500 | 1347 | 618 | 57.60 | .5293 | 301.4 |
| 17 | | 732 | .5187 | .7105 | 80.77 | 32.0 | 4.3 | .01714 | 1395 | 663 | 54.58 | .5337 | 301.4 |
| 18 | | 722 | .5187 | .7105 | 79.70 | 37.5 | 4.3 | .02009 | 1452 | 730 | 51.77 | .5282 | 301.4 |
| 19 | | 729 | .5187 | .7105 | 80.46 | 45.2 | 4.3 | .02421 | 1528 | 799 | 47.80 | .5307 | 301.4 |
| 20 | | 722 | .5187 | .7105 | 79.70 | 60.0 | 4.3 | .03214 | 1633 | 911 | 42.11 | .5502 | 301.4 |
| 21 | 8.0 | 730 | .8327 | 1.141 | 80.82 | 25.8 | --- | .008606 | 1282 | 552 | 87.77 | .7400 | 189.1 |
| 22 | | 726 | .8307 | 1.138 | 80.26 | 41.4 | --- | .01384 | 1565 | 839 | 85.47 | .8179 | 188.6 |
| 23 | | 730 | .8341 | 1.143 | 80.97 | 21.0 | --- | .006993 | 1174 | 444 | 85.96 | .7871 | 189.4 |
| 24 | | 728 | .8292 | 1.136 | 80.26 | 31.0 | --- | .01039 | 1382 | 654 | 87.00 | .8012 | 188.2 |
| 25 | 5.0 | 729 | .5173 | .7086 | 80.26 | 21.2 | 3.3 | .01139 | 1262 | 533 | 64.47 | .4918 | 300.6 |
| 26 | | 732 | .5281 | .7234 | 82.24 | 23.6 | 3.8 | .01241 | 1275 | 543 | 60.50 | .5282 | 306.8 |
| 27 | | 722 | .5222 | .7153 | 80.21 | 21.5 | 3.3 | .01144 | 1231 | 509 | 61.20 | .5076 | 303.4 |
| 28 | | 728 | .5203 | .7127 | 80.71 | 27.0 | 4.0 | .01442 | 1331 | 603 | 58.32 | .5592 | 302.3 |
| 29 | | 734 | .5227 | .7160 | 81.78 | 32.4 | 4.3 | .01722 | 1408 | 674 | 55.31 | .5548 | 303.7 |
| 30 | | 728 | .5222 | .7153 | 81.02 | 36.9 | 4.3 | .01963 | 1404 | 676 | 48.92 | .5538 | 303.4 |
| 10.5 gal/hr, 60° fuel atomizer; fuel, heated JP-4 | | | | | | | | | | | | | |
| 31 | 15.0 | 720 | 1.555 | 2.130 | 79.29 | 36.6 | 19.0 | 0.006538 | 1167 | 447 | 92.31 | 1.252 | $100.4\times10^{-6}$ |
| 32 | 15.05 | 732 | 1.554 | 2.129 | 80.31 | 48.2 | 20.1 | .008616 | 1328 | 596 | 94.91 | 1.335 | 99.70 |
| 33 | 15.0 | 725 | 1.553 | 2.127 | 79.75 | 53.7 | 22.1 | .009605 | 1387 | 662 | 95.04 | 1.351 | 100.2 |
| 34 | | 733 | 1.553 | 2.127 | 80.61 | 63.9 | 22.8 | .01143 | 1498 | 765 | 93.45 | 1.376 | 100.2 |
| 35 | | 733 | 1.556 | 2.132 | 80.87 | 74.4 | 23.9 | .01328 | 1628 | 895 | 95.29 | 1.438 | 100.5 |
| 36 | | 730 | 1.557 | 2.133 | 80.51 | 87.2 | 24.7 | .01556 | 1764 | 1034 | 95.19 | 1.489 | 100.5 |
| 37 | | 733 | 1.566 | 2.145 | 81.37 | 103.9 | 26.5 | .01843 | 1960 | 1227 | 97.21 | 1.551 | 101.1 |
| 38 | 8.0 | 728 | .8347 | 1.143 | 80.77 | 20.7 | 11.9 | .006889 | 1150 | 422 | 82.84 | .7385 | 189.4 |
| 39 | | 725 | .8337 | 1.142 | 80.41 | 25.8 | 13.7 | .008597 | 1278 | 553 | 87.94 | .7900 | 189.2 |
| 40 | | 731 | .8298 | 1.137 | 80.66 | 31.6 | 14.3 | .01058 | 1384 | 653 | 85.39 | .8089 | 188.4 |
| 41 | | 729 | .8354 | 1.144 | 81.07 | 36.9 | 16.0 | .01227 | 1494 | 765 | 87.23 | .8262 | 189.5 |
| 42 | | 734 | .8335 | 1.142 | 81.42 | 43.3 | 19.1 | .01443 | 1622 | 888 | 87.25 | .8710 | 189.2 |
| 43 | | 736 | .8335 | 1.142 | 81.63 | 50.3 | 20.8 | .01676 | 1726 | 990 | 84.81 | .8675 | 189.2 |
| 44 | | 730 | .8305 | 1.138 | 80.71 | 58.0 | 26.4 | .01940 | 1826 | 1096 | 82.06 | .8907 | 188.6 |
| 45 | | 722 | .8266 | 1.132 | 79.40 | 75.8 | 26.9 | .02547 | 1974 | 1252 | 73.11 | .9082 | 187.6 |
| 46 | 5.0 | 730 | .5187 | .7105 | 80.56 | 20.0 | 13.5 | .01071 | 1271 | 541 | 69.48 | .5132 | 301.4 |
| 47 | | 722 | .5187 | .7105 | 79.70 | 27.0 | 17.5 | .01446 | 1489 | 767 | 74.56 | .5700 | 301.4 |
| 48 | | 735 | .5187 | .7105 | 81.12 | 33.5 | 20.5 | .01794 | 1556 | 821 | 65.26 | .5741 | 301.4 |
| 49 | | 723 | .5183 | .7100 | 79.75 | 38.6 | 22.3 | .02069 | 1661 | 938 | 65.44 | .5796 | 301.2 |
| 50 | | 728 | .5183 | .7100 | 80.26 | 45.0 | ---- | .02412 | 1707 | 979 | 59.31 | .5838 | 301.2 |
| 10.5 gal/hr, 60° fuel atomizer; fuel, propane | | | | | | | | | | | | | |
| 51 | 8.0 | 723 | 0.8342 | 1.143 | 80.21 | 25.26 | ---- | 0.008412 | 1310 | 587 | 90.02 | 0.7864 | $189.4\times10^{-6}$ |
| 52 | | 714 | .8312 | 1.139 | 78.94 | 28.96 | ---- | .009679 | 1374 | 660 | 88.58 | .7922 | 188.7 |
| 53 | | 720 | .8302 | 1.137 | 79.45 | 31.03 | ---- | .01038 | 1426 | 706 | 88.87 | .8096 | 188.4 |
| 54 | | 724 | .8342 | 1.143 | 80.31 | 33.40 | ---- | .01112 | 1477 | 753 | 88.93 | .8630 | 189.4 |
| 55 | | 728 | .8322 | 1.140 | 80.56 | 36.23 | ---- | .01209 | 1538 | 810 | 88.61 | .8720 | 188.9 |
| 56 | 5.0 | 722 | .5380 | .7370 | 82.89 | 19.85 | ---- | .01025 | 1345 | 623 | 79.02 | .5880 | 312.6 |
| 57 | | 718 | .5142 | .7044 | 78.53 | 22.67 | ---- | .01225 | 1442 | 724 | 77.69 | .5799 | 298.8 |
| 58 | | 722 | .5221 | .7152 | 80.31 | 23.97 | ---- | .01275 | 1507 | 785 | 81.40 | .6051 | 303.4 |
| 59 | | 723 | .5221 | .7152 | 80.46 | 27.64 | ---- | .01470 | 1574 | 851 | 77.33 | .6149 | 303.4 |
| 60 | | 723 | .5231 | .7166 | 80.61 | 29.59 | ---- | .01571 | 1654 | 931 | 79.75 | .6241 | 304.0 |
| 61 | | 723 | .5221 | .7152 | 80.46 | 32.53 | ---- | .01730 | 1714 | 991 | 77.72 | .6698 | 303.4 |
| 62 | | 735 | .5251 | .7193 | 82.24 | 35.64 | ---- | .01886 | 1777 | 1042 | 75.65 | .6739 | 305.2 |
| 63 | | 727 | .5226 | .7159 | 80.97 | 38.29 | ---- | .02036 | 1876 | 1149 | 77.99 | .6588 | 303.7 |
| 30.0 gal/hr, 70° fuel atomizer; fuel, propane | | | | | | | | | | | | | |
| 64 | 15.0 | 724 | 1.558 | 2.134 | 79.80 | 45.17 | ---- | 0.008053 | 1326 | 602 | 96.38 | 1.507 | $100.6\times10^{-6}$ |
| 65 | | 728 | 1.560 | 2.137 | 80.36 | 51.63 | ---- | .009193 | 1420 | 692 | 98.02 | 1.584 | 100.7 |
| 66 | | 734 | 1.559 | 2.136 | 81.02 | 57.97 | ---- | .01033 | 1498 | 764 | 97.09 | 1.608 | 100.7 |
| 67 | | 722 | 1.560 | 2.137 | 79.70 | 65.48 | ---- | .01166 | 1587 | 865 | 98.21 | 1.629 | 100.7 |
| 68 | | 732 | 1.560 | 2.137 | 80.82 | 72.03 | ---- | .01283 | 1669 | 937 | 97.56 | 1.659 | 100.7 |
| 69 | | 723 | 1.560 | 2.137 | 79.80 | 83.47 | ---- | .01486 | 1803 | 1080 | 98.34 | 1.665 | 100.7 |
| 70 | | 722 | 1.560 | 2.137 | 79.70 | 95.05 | ---- | .01692 | 1916 | 1194 | 95.95 | 1.685 | 100.7 |
| 71 | 8.0 | 726 | .8349 | 1.144 | 80.56 | 23.51 | ---- | .007821 | 1246 | 520 | 85.36 | .8586 | 189.5 |
| 72 | | 732 | .8310 | 1.138 | 80.82 | 27.64 | ---- | .009238 | 1347 | 615 | 86.39 | .8924 | 188.6 |
| 73 | | 731 | .8359 | 1.145 | 81.22 | 32.26 | ---- | .01072 | 1441 | 710 | 86.80 | .9259 | 189.7 |

TABLE II - DATA OBTAINED FOR MODEL 13 COMBUSTOR - Concluded

| Run | Combustor-inlet total pressure $P_1$ (in. Hg) | Combustor-inlet total temperature $T_1$ ($^\circ$R) | Air flow rate $W_a$ (lb/sec) | Air flow rate per unit area $W_a/A_r$ $\left(\frac{lb}{(sec)(sq\ ft)}\right)$ | Combustor reference velocity $V_r$ (ft/sec) | Fuel flow rate $W_f$ (lb/hr) | Fuel manifold pressure (above combustor-inlet pressure) $\Delta P_f$ (lb/sq in.) | Fuel-air ratio f | Mean combustor-outlet temperature $T_0$ ($^\circ$R) | Mean temperature rise through combustor $\Delta T$ ($^\circ$F) | Combustion efficiency $\eta_b$ (percent) | Total pressure drop through combustor $\Delta P$ (in. Hg) | Combustion parameter $V_r/p_1T_1$ (ft, lb, sec, $^\circ$R units) |
|---|---|---|---|---|---|---|---|---|---|---|---|---|---|
| 30.0 gal/hr, 70° fuel atomizer; fuel, propane - concluded | | | | | | | | | | | | | |
| 74 | | 728 | .8338 | 1.142 | 80.66 | 43.62 | ---- | .01453 | 1684 | 956 | 88.40 | .9783 | 189.2x10$^{-6}$ |
| 75 | | 728 | .8338 | 1.142 | 80.56 | 51.63 | ---- | .01720 | 1813 | 1085 | 86.05 | 1.014 | 189.2 |
| 76 | | 733 | .8308 | 1.138 | 80.92 | 55.58 | ---- | .01858 | 1899 | 1166 | 86.42 | 1.006 | 188.6 |
| 77 | 5.0 | 732 | .5179 | .7095 | 80.77 | 20.88 | ---- | .01120 | 1358 | 626 | 73.01 | .5946 | 300.9 |
| 78 | | 726 | .5228 | .7162 | 80.87 | 24.29 | ---- | .01291 | 1472 | 746 | 76.33 | .6512 | 303.8 |
| 79 | | 726 | .5218 | .7148 | 80.61 | 28.56 | ---- | .01521 | 1580 | 854 | 75.13 | .6580 | 303.2 |
| 80 | | 733 | .5218 | .7148 | 81.37 | 32.37 | ---- | .01724 | 1724 | 991 | 78.08 | .6849 | 303.2 |
| 81 | | 728 | .5228 | .7162 | 80.97 | 35.44 | ---- | .01883 | 1809 | 1081 | 78.68 | .6853 | 303.8 |
| 82 | | 733 | .5228 | .7162 | 81.53 | 39.18 | ---- | .02082 | 1865 | 1132 | 75.24 | .6747 | 303.8 |
| 83 | | 733 | .5233 | .7168 | 81.73 | 42.30 | ---- | .02245 | 1776 | 1043 | 64.27 | .6587 | 304.0 |
| 84 | | 726 | .5218 | .7148 | 82.29 | 39.24 | ---- | .02420 | 1652 | 926 | 52.80 | .5943 | 315.7 |
| 3.0 gal/hr, 60° fuel atomizer; fuel, JP-4 | | | | | | | | | | | | | |
| 85 | 15.0 | 722 | 1.561 | 2.138 | 79.70 | 35.0 | 8.5 | 0.006228 | 1180 | 458 | 99.23 | 1.360 | 100.8x10$^{-6}$ |
| 86 | | 728 | 1.558 | 2.134 | 80.26 | 47.0 | 9.8 | .008379 | 1323 | 595 | 97.26 | 1.408 | 100.6 |
| 87 | | 720 | 1.559 | 2.136 | 79.35 | 52.9 | 11.3 | .009426 | 1407 | 687 | 100.5 | 1.432 | 100.7 |
| 88 | | 726 | 1.558 | 2.134 | 80.00 | 64.0 | 13.0 | .01141 | 1545 | 819 | 100.4 | 1.494 | 100.6 |
| 89 | | 722 | 1.563 | 2.141 | 79.80 | 73.6 | 17.0 | .01308 | 1644 | 922 | 99.59 | 1.546 | 100.9 |
| 90 | | 726 | 1.559 | 2.136 | 80.06 | 84.9 | 23.3 | .01513 | 1751 | 1025 | 96.85 | 1.541 | 100.7 |
| 91 | | 732 | 1.558 | 2.134 | 80.71 | 103.0 | 35.7 | .01836 | 1849 | 1117 | 88.26 | 1.465 | 100.6 |
| 92 | 8.0 | 721 | .8369 | 1.146 | 80.31 | 22.4 | 8.1 | .007434 | 1208 | 487 | 88.92 | .7676 | 189.9 |
| 93 | | 727 | .8359 | 1.145 | 80.82 | 25.7 | 9.7 | .008541 | 1255 | 528 | 84.41 | .7856 | 189.7 |
| 94 | | 732 | .8369 | 1.146 | 81.58 | 29.3 | 10.1 | .009725 | 1349 | 617 | 87.41 | .8421 | 189.9 |
| 95 | | 732 | .8349 | 1.144 | 81.27 | 38.2 | 9.4 | .01271 | 1524 | 792 | 87.42 | .8739 | 189.5 |
| 96 | | 725 | .8340 | 1.142 | 80.41 | 43.4 | 9.6 | .01446 | 1618 | 893 | 87.46 | .8768 | 189.2 |
| 97 | | 726 | .8330 | 1.141 | 80.41 | 49.7 | 10.7 | .01657 | 1739 | 1013 | 87.67 | .8926 | 189.1 |
| 98 | | 728 | .8320 | 1.140 | 80.51 | 62.0 | 11.7 | .02070 | 1817 | 1089 | 76.62 | .8837 | 188.9 |
| 99 | | 723 | .8343 | 1.143 | 80.21 | 69.7 | 15.0 | .02321 | 1806 | 1083 | 68.36 | .8108 | 189.4 |
| 100 | 5.0 | 728 | .5233 | .7168 | 81.32 | 20.3 | 9.7 | .01077 | 1202 | 474 | 60.38 | .4888 | 304.0 |
| 101 | | 727 | .5243 | .7182 | 81.32 | 24.8 | 9.7 | .01314 | 1268 | 541 | 57.02 | .5059 | 304.6 |
| 102 | | 722 | .5243 | .7182 | 80.66 | 31.8 | 10.1 | .01685 | 1332 | 610 | 50.78 | .5077 | 304.6 |
| 103 | | 726 | .5243 | .7182 | 81.12 | 40.9 | 10.5 | .02167 | 1453 | 727 | 48.03 | .4996 | 304.6 |
| 104 | | 730 | .5223 | .7155 | 81.22 | 44.2 | 9.5 | .02351 | 1404 | 674 | 41.17 | .5390 | 303.5 |
| 105 | | 730 | .5223 | .7155 | 81.22 | 50.0 | --- | ------ | ---- | Blow-out | | ----- | ----- |
| 10.5 gal/hr, 60° fuel atomizer; fuel, JP-4 | | | | | | | | | | | | | |
| 106 | 15.0 | 730 | 2.0355 | 2.788 | 107.6 | 55.2 | 6.2 | 0.007533 | 1288 | 558 | 101.03 | 2.4405 | 131.4x10$^{-6}$ |
| 107 | | 726 | 2.0306 | 2.782 | 106.8 | 65.0 | 6.4 | .008892 | 1375 | 649 | 100.38 | 2.5055 | 131.1 |
| 108 | | 724 | 2.0355 | 2.788 | 106.7 | 76.6 | 6.3 | .01045 | 1483 | 759 | 100.97 | 2.6688 | 131.4 |
| 109 | | 722 | 2.0336 | 2.786 | 106.3 | 88.0 | 6.3 | .01202 | 1564 | 842 | 98.20 | 2.7275 | 131.3 |
| 110 | | 724 | 2.0231 | 2.771 | 106.1 | 94.5 | 6.4 | .01298 | 1636 | 912 | 99.22 | 2.7656 | 130.6 |
| 111 | | 723 | 2.0339 | 2.786 | 106.5 | 93.3 | 6.5 | .01274 | 1621 | 898 | 99.37 | 2.7908 | 131.3 |
| 112 | | 732 | 2.0345 | 2.787 | 107.8 | 101.0 | 6.5 | .01379 | 1698 | 966 | 99.52 | 2.8439 | 131.4 |
| 113 | | 728 | 2.0335 | 2.786 | 107.2 | 119.7 | 6.5 | .01635 | 1851 | 1123 | 99.10 | 2.9195 | 131.3 |
| 114 | | 734 | 2.0275 | 2.777 | 107.7 | 130.5 | 6.4 | .01788 | 1955 | 1221 | 99.51 | 2.9194 | 130.9 |
| 115 | | 732 | 2.630 | 3.603 | 145.0 | 72.3 | --- | .007636 | 1257 | 525 | 93.70 | 4.611 | 169.8 |
| 116 | | 728 | 2.633 | 3.607 | 144.3 | 92.4 | --- | .009748 | 1392 | 664 | 94.02 | 4.803 | 170.0 |
| 117 | | 731 | 2.623 | 3.593 | ----- | 110.5 | --- | .01170 | 1522 | 791 | 94.56 | ----- | 169.3 |
| 118 | | 730 | 2.625 | 3.596 | ----- | 132.7 | --- | .01404 | 1630 | 900 | 90.78 | ----- | 169.5 |
| 119 | | 723 | 2.623 | 3.593 | ----- | 149.0 | --- | .01578 | 1652 | 929 | 83.80 | ----- | 169.3 |
| 120 | | 723 | 2.626 | 3.597 | ----- | 168.8 | --- | .01785 | 1563 | 840 | 67.05 | ----- | 169.5 |
| 121 | 15.05 | 734 | 2.623 | 3.593 | ----- | 188.9 | --- | .02000 | 1502 | 768 | 54.92 | ----- | 168.2 |
| 30.0 gal/hr, 70° fuel atomizer; fuel, propane | | | | | | | | | | | | | |
| 122 | 15.0 | 726 | 2.029 | 2.779 | 106.5 | 51.76 | --- | 0.007087 | 1266 | 540 | 97.70 | 2.694 | 131.0x10$^{-6}$ |
| 123 | | 734 | 2.027 | 2.777 | 107.5 | 57.96 | --- | .007943 | 1356 | 622 | 101.2 | 2.907 | 130.9 |
| 124 | | 730 | 2.030 | 2.781 | 107.0 | 69.42 | --- | .009499 | 1445 | 715 | 98.27 | 3.004 | 131.1 |
| 125 | | 720 | 2.029 | 2.779 | 105.6 | 81.20 | --- | .01112 | 1527 | 807 | 95.55 | 3.021 | 131.0 |
| 126 | | 723 | 2.029 | 2.779 | 106.0 | 87.67 | --- | .01200 | 1621 | 898 | 99.37 | 3.072 | 131.0 |
| 127 | | 732 | 2.030 | 2.781 | 107.3 | 99.32 | --- | .01359 | 1728 | 996 | 98.47 | 3.118 | 131.1 |
| 128 | | 724 | 2.029 | 2.779 | 106.2 | 109.6 | --- | .01501 | 1824 | 1100 | 99.34 | 3.104 | 131.0 |
| 129 | | 734 | 2.029 | 2.779 | 107.6 | 114.9 | --- | .01573 | 1891 | 1157 | 100.4 | 3.215 | 131.0 |
| 130 | | 734 | 2.594 | 3.553 | ----- | 84.27 | --- | .006883 | 1286 | 552 | 102.9 | ----- | 167.4 |
| 131 | 15.1 | 732 | 2.606 | 3.570 | ----- | 78.06 | --- | .008320 | 1351 | 619 | 96.24 | ----- | 166.0 |
| 132 | 15.2 | 730 | 2.607 | 3.571 | ----- | 96.72 | --- | .01031 | 1469 | 739 | 93.89 | ----- | 163.9 |
| 133 | 15.6 | 732 | 2.619 | 3.588 | ----- | 108.5 | --- | .01151 | 1569 | 837 | 96.22 | ----- | 156.3 |
| 134 | 15.65 | 722 | 2.617 | 3.585 | ----- | 116.5 | --- | .01237 | 1612 | 890 | 95.56 | ----- | 155.2 |
| 60.0 gal/hr, 70° fuel atomizer; fuel, propane | | | | | | | | | | | | | |
| 135 | 15.0 | 729 | 2.622 | 3.592 | 143.2 | 80.19 | --- | 0.008496 | 1377 | 648 | 98.82 | ------ | 169.3x10$^{-6}$ |
| 136 | 15.1 | 727 | 2.624 | 3.595 | 141.8 | 105.8 | --- | .01120 | 1551 | 824 | 97.08 | ------ | 167.2 |
| 137 | 15.4 | 727 | 2.612 | 3.578 | 137.9 | 130.9 | --- | .01392 | 1727 | 1000 | 96.53 | ------ | 160.0 |
| 138 | 15.5 | 726 | 2.618 | 3.586 | 137.1 | 156.9 | --- | .01665 | 1857 | 1131 | 92.73 | ------ | 158.3 |
| 139 | 15.25 | 724 | 2.601 | 3.563 | 138.2 | 180.3 | --- | .01925 | 1854 | 1130 | 80.71 | ------ | 162.5 |
| 140 | 15.5 | 728 | 2.591 | 3.549 | ----- | 192.5 | --- | .02064 | 7918 | 1190 | 79.94 | ------ | 156.6 |
| 141 | 15.2 | 726 | 2.607 | 3.571 | ----- | 198.6 | --- | .02116 | 1851 | 1125 | 73.55 | ------ | 163.9 |
| 142 | 15.0 | 722 | 2.621 | 3.590 | 142.2 | ----- | --- | ------ | ---- | ---- | ----- | 3.074 | 169.2 |
| 143 | 15.0 | 724 | 2.0349 | 2.788 | 106.7 | ----- | --- | ------ | ---- | ---- | ----- | 1.652 | 131.4 |
| 144 | 8.0 | 728 | .8349 | 1.144 | 80.92 | ----- | --- | ------ | ---- | ---- | ----- | .5294 | 189.5 |
| 145 | 5.0 | 731 | .5226 | .7159 | 81.42 | ----- | --- | ------ | ---- | ---- | ----- | .3590 | 303.7 |

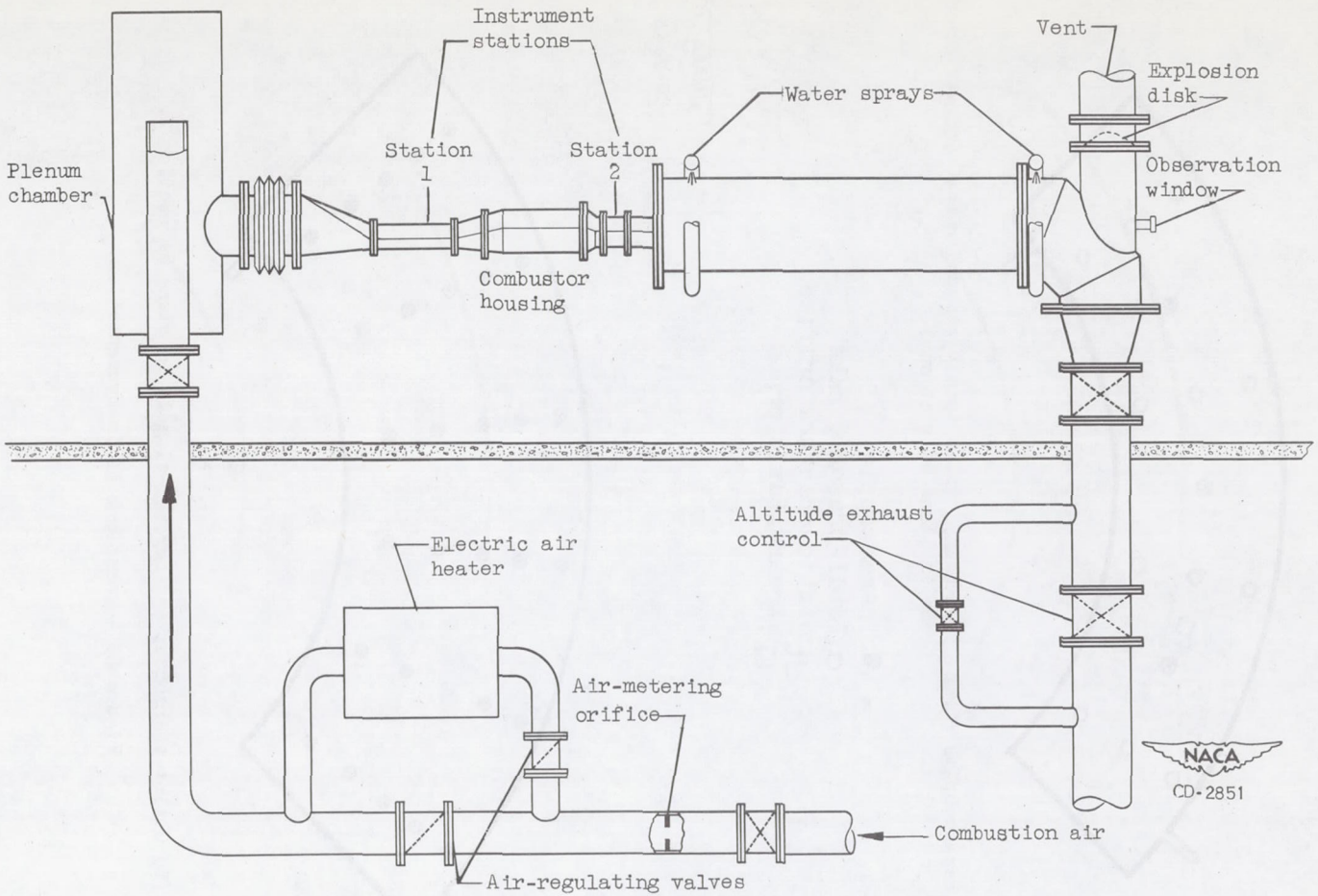


Figure 1. - Installation of one-quarter sector of $25\frac{1}{2}$-inch-diameter annular combustor.

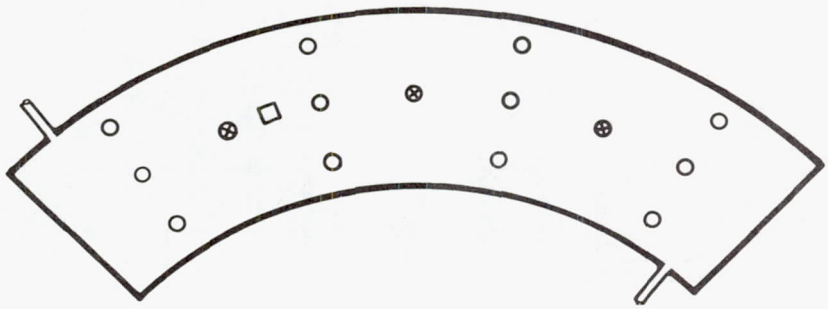

(a) Inlet thermocouples (iron-constantan), inlet total-pressure rakes, and stream-static probe in plane at station 1.

⊗ Thermocouple
O Total-pressure rake
Static-pressure orifice
□ Stream-static probe

NACA
CD-2845

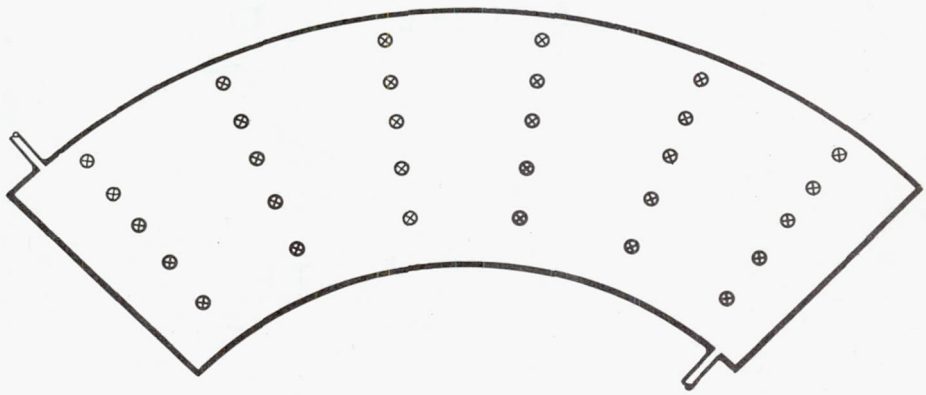

(b) Outlet thermocouples (chromel-alumel) in plane at station 2.

Figure 2. - Locations of instrumentation.

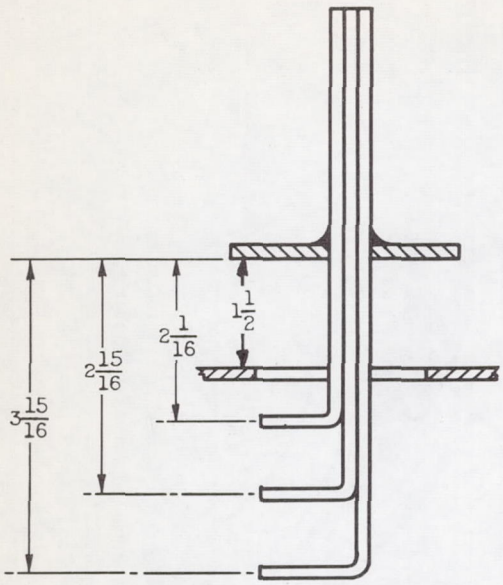


(a) Inlet total-pressure rake.

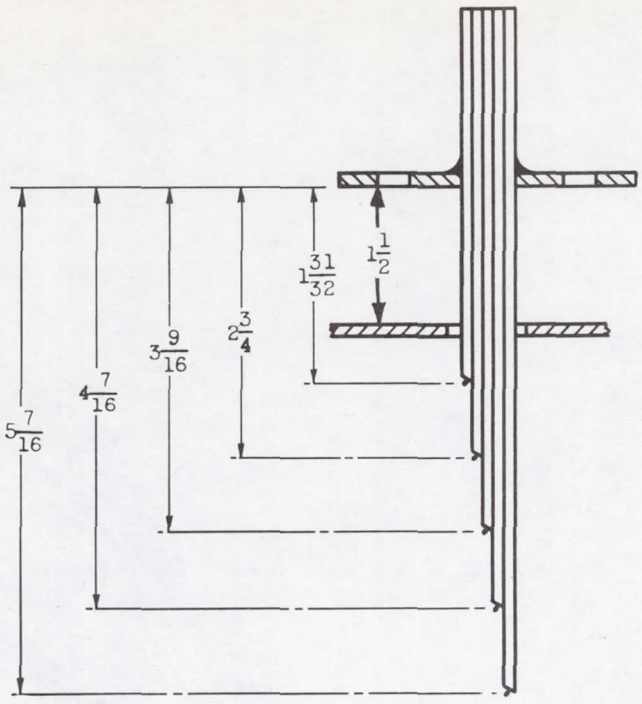


(b) Outlet thermocouple rake.

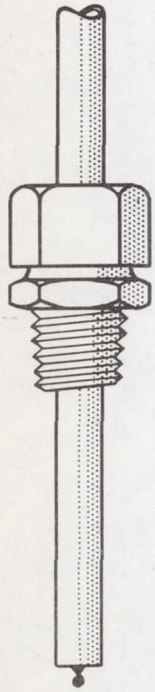

(c) Inlet thermocouple.

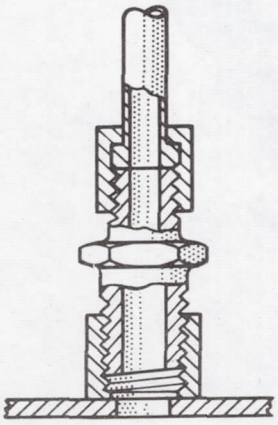

(d) Static-pressure orifice.

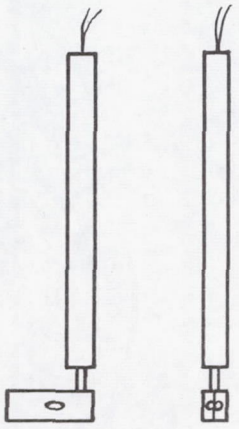

(e) Wedge stream-static probe.

NACA

CD-2846

Figure 3. - Details of instrumentation. (Dimensions are in inches.)

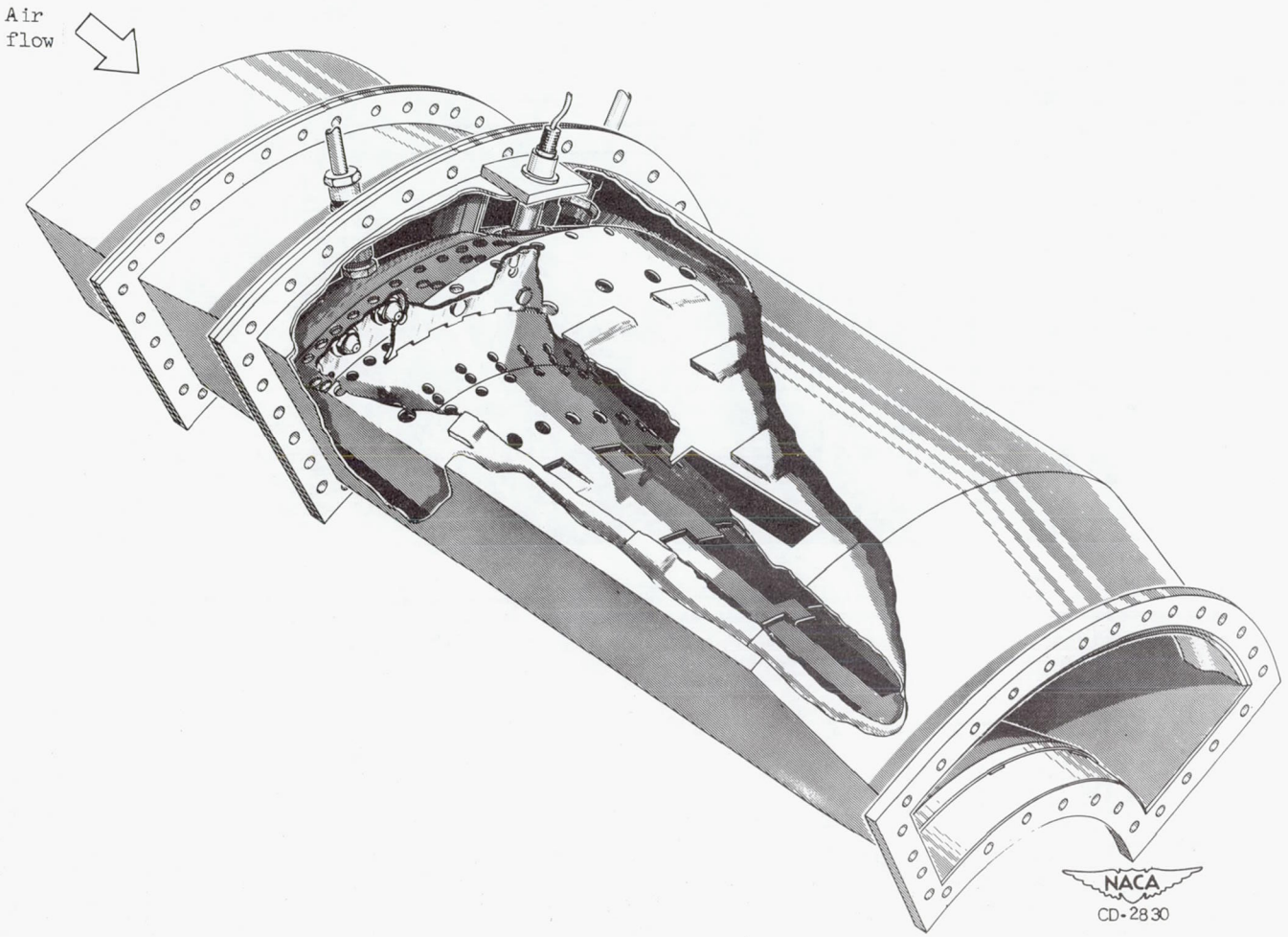


Figure 4. - One-quarter sector of model 13 annular combustor assembled in test ducting.

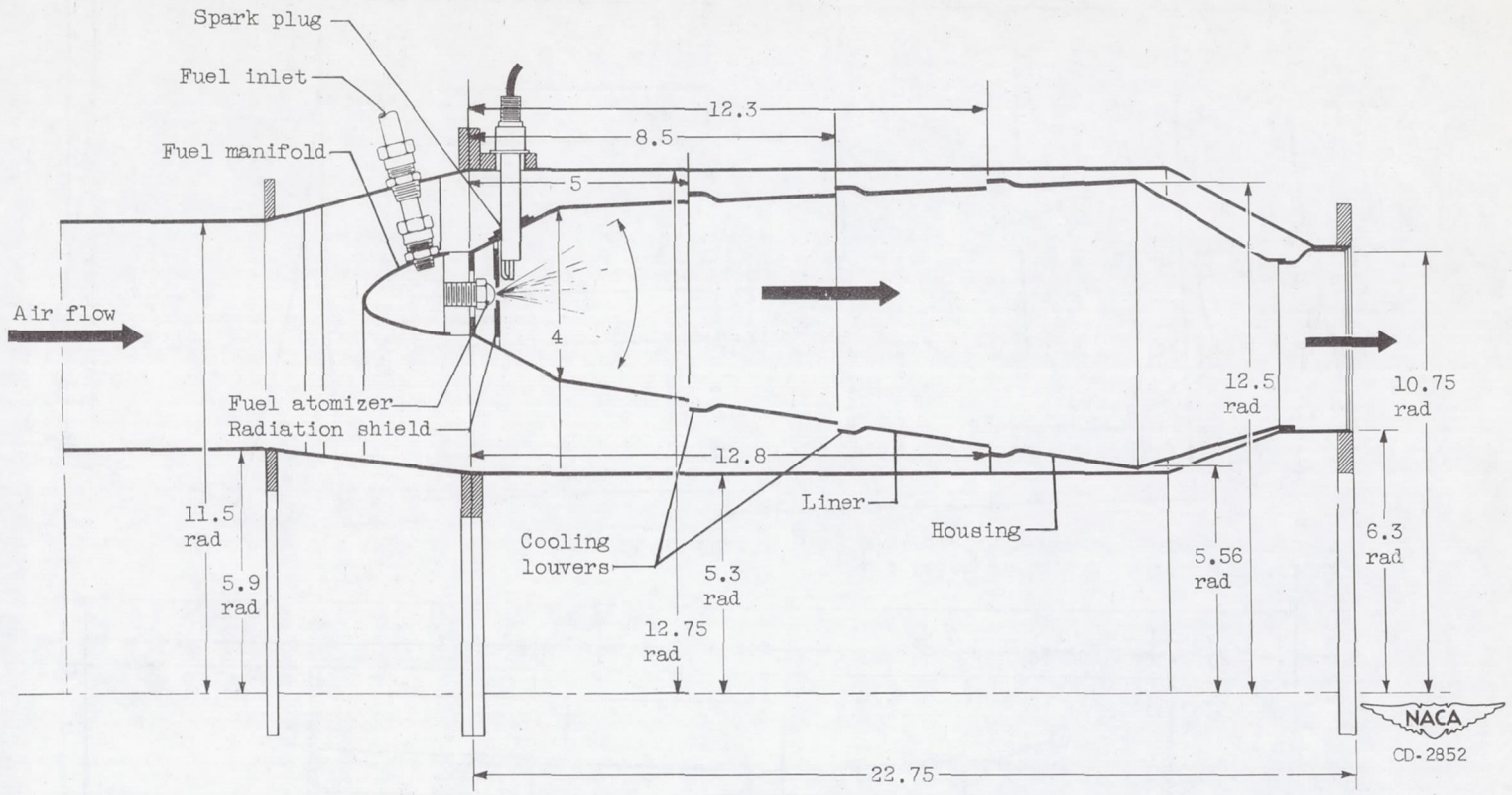


Figure 5. - Longitudinal cross-sectional view of combustor and housing. (Dimensions are in inches.)

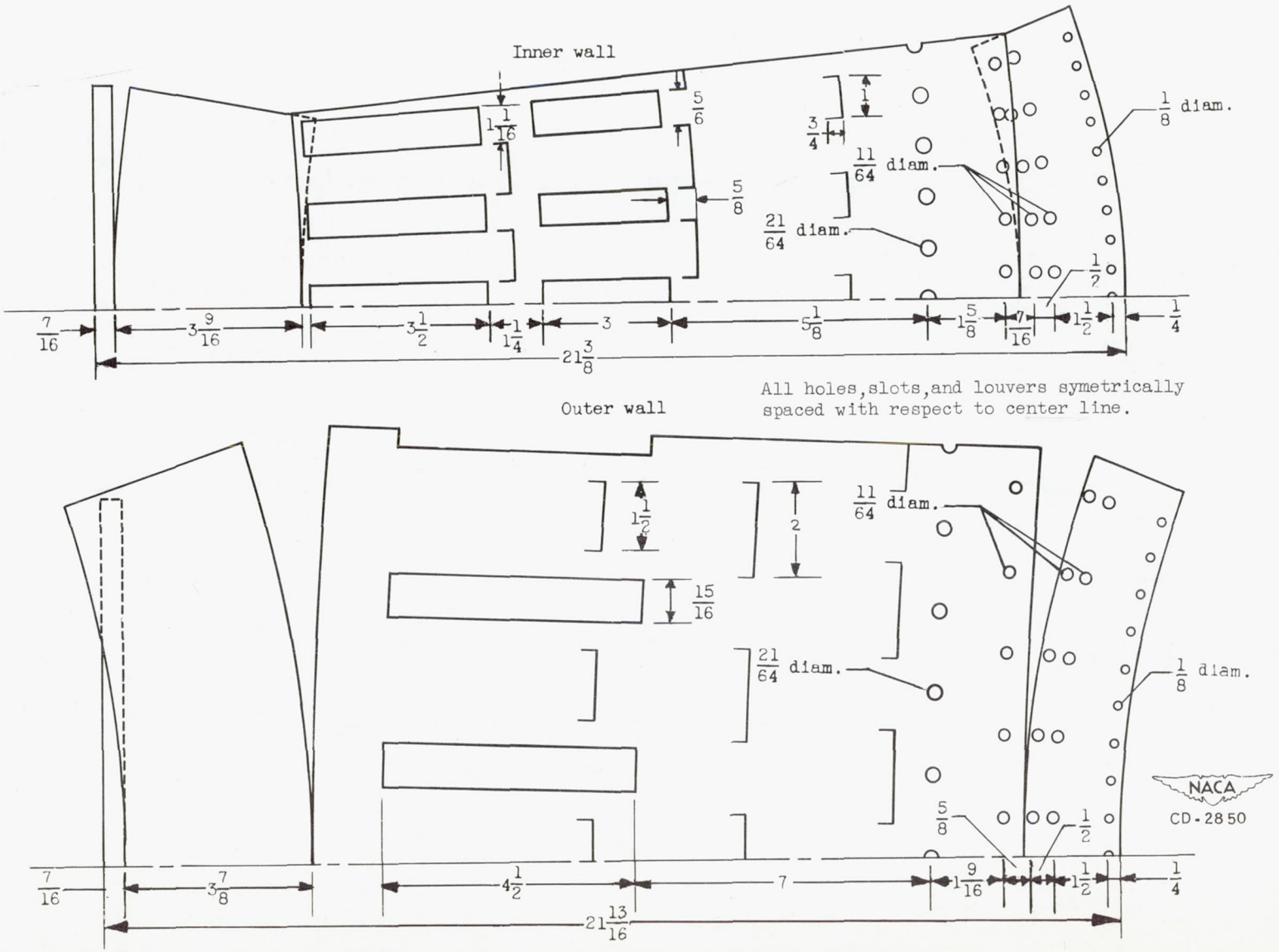


Figure 6. - One-eighth sector developed view of liner walls of combustor model 13. (Dimensions are in inches.)

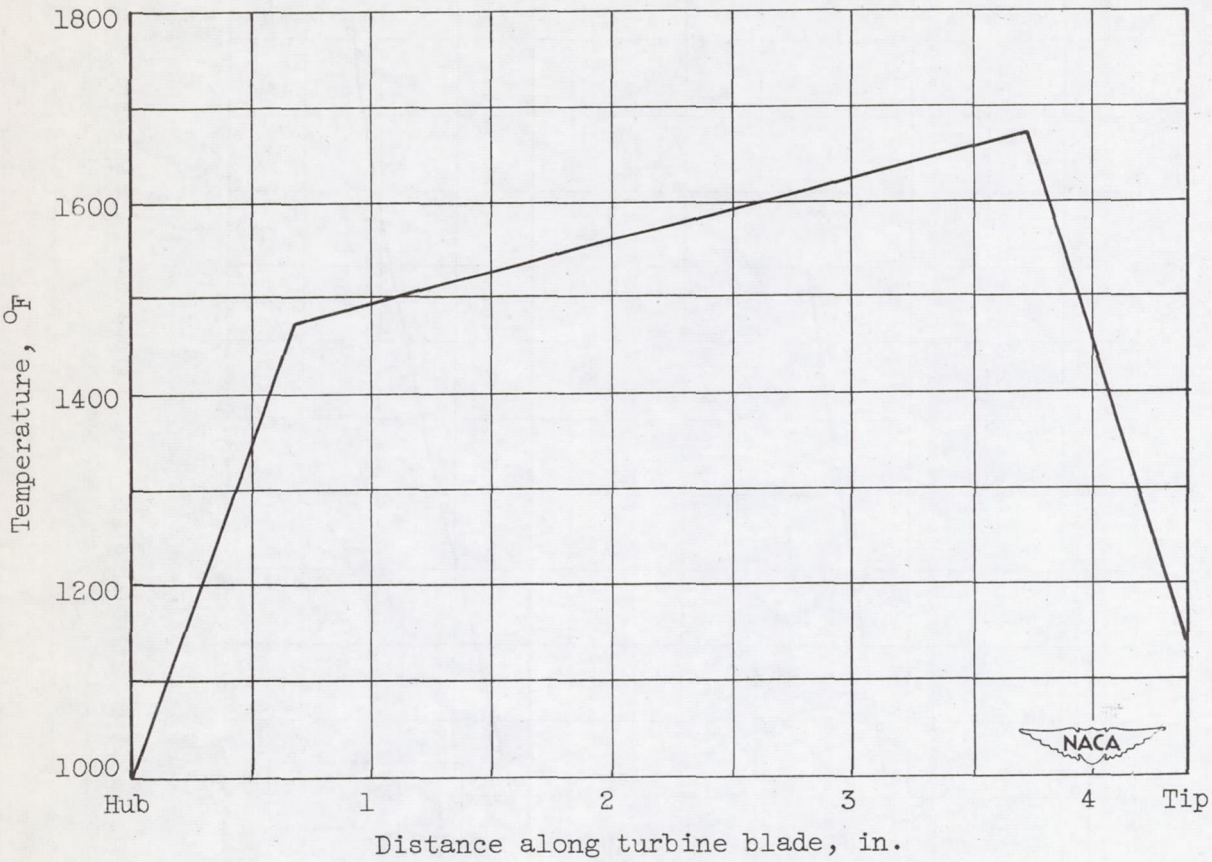


Figure 7. - Desired combustor-outlet temperature distribution.

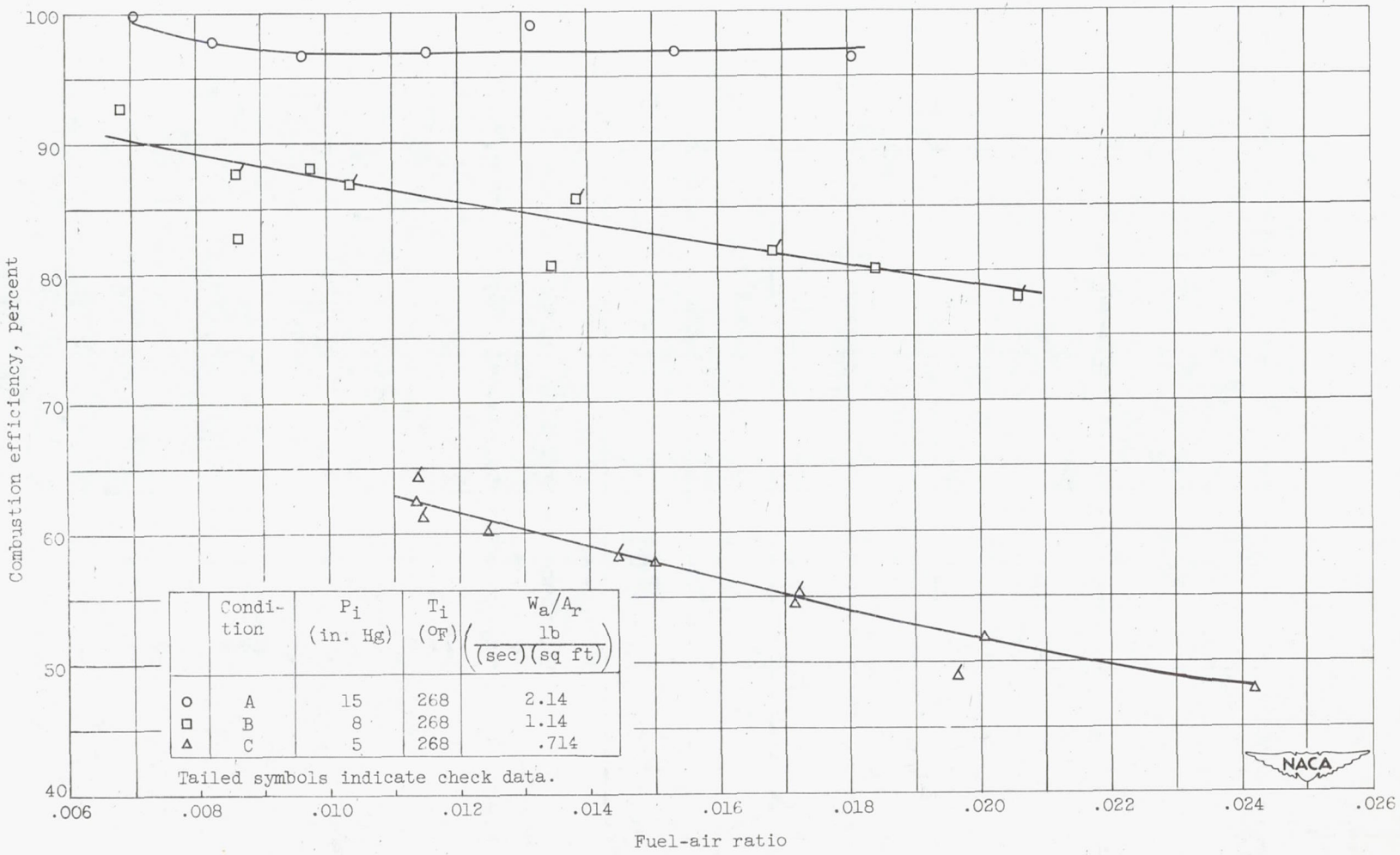


Figure 8. - Combustion efficiency of model 13 combustor with liquid MIL-F-5624A grade JP-4 fuel at various pressures. 10.5-gallon-per-hour, 60° fuel atomizers.

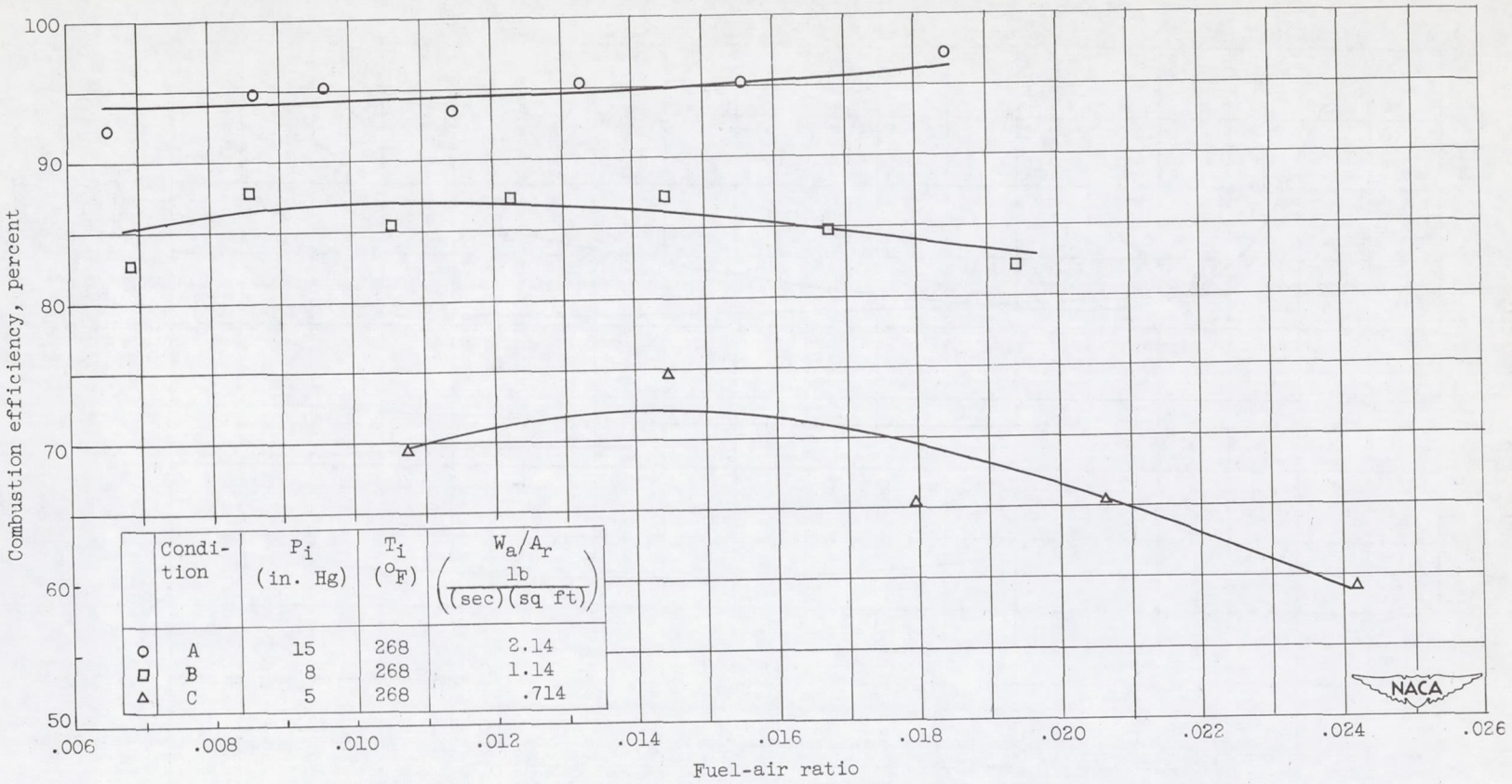


Figure 9. - Combustion efficiency of model 13 combustor with heated (300° F) MIL-F-5624A grade JP-4 fuel at various pressures. 10.5-gallon-per-hour, 60° fuel atomizers.

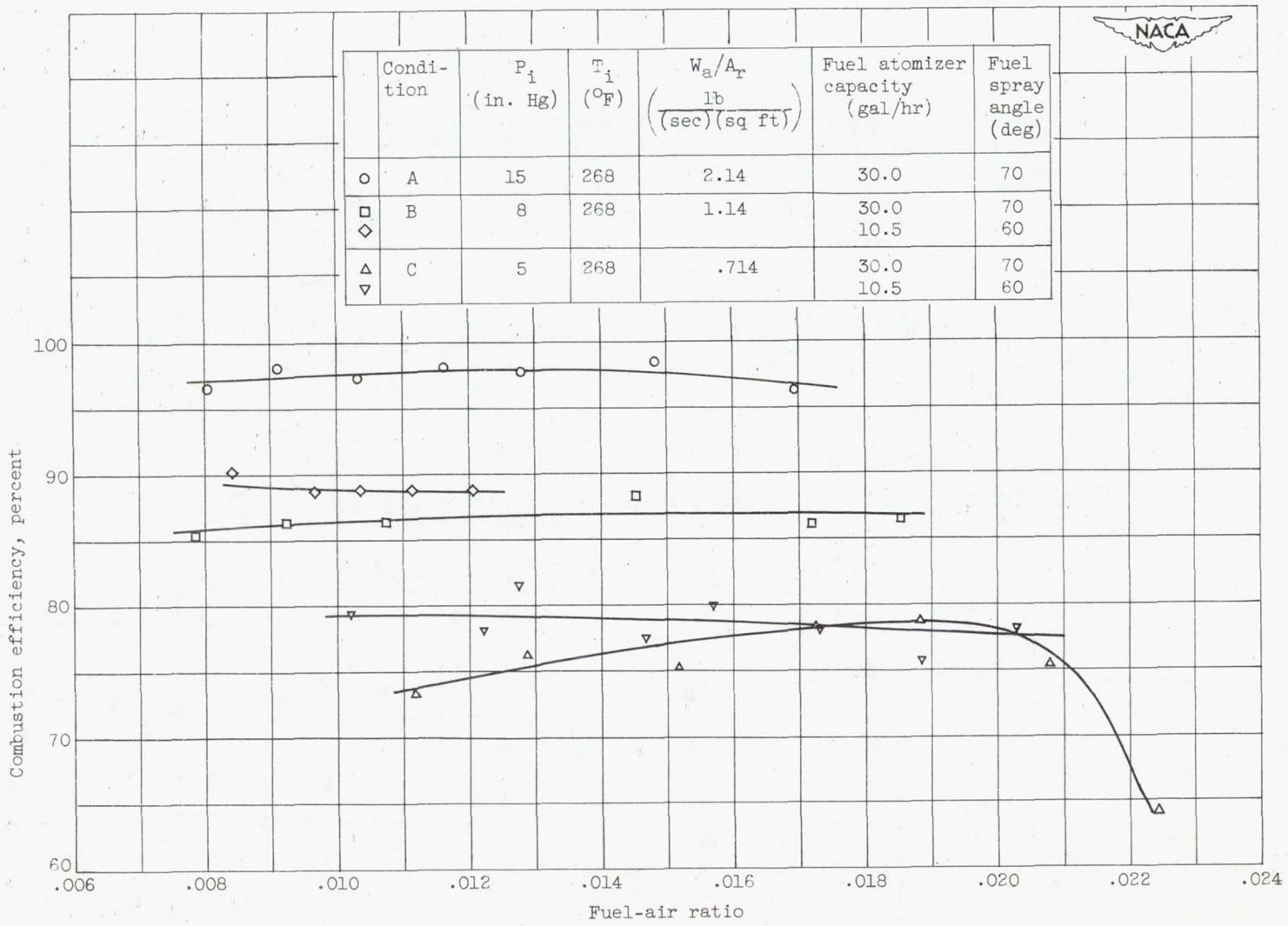


Figure 10. - Combustion efficiency of model 13 combustor with vapor (propane) fuel at various pressures. Two fuel atomizer capacities.

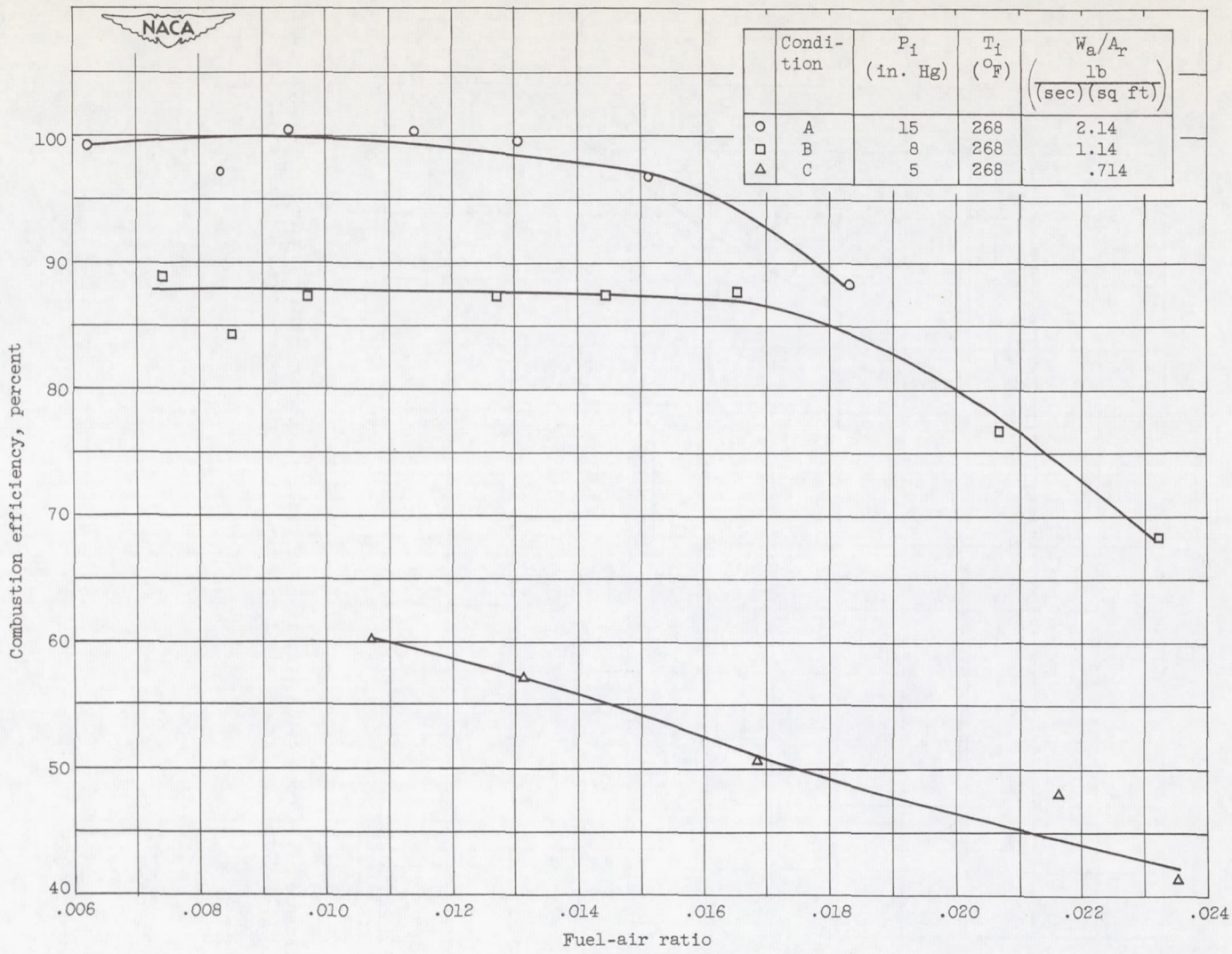


Figure 11. - Combustion efficiency of model 13 combustor with liquid MIL-F-5624A grade JP-4 fuel at various pressures. 3.0-gallon-per-hour, 60° fuel atomizers.

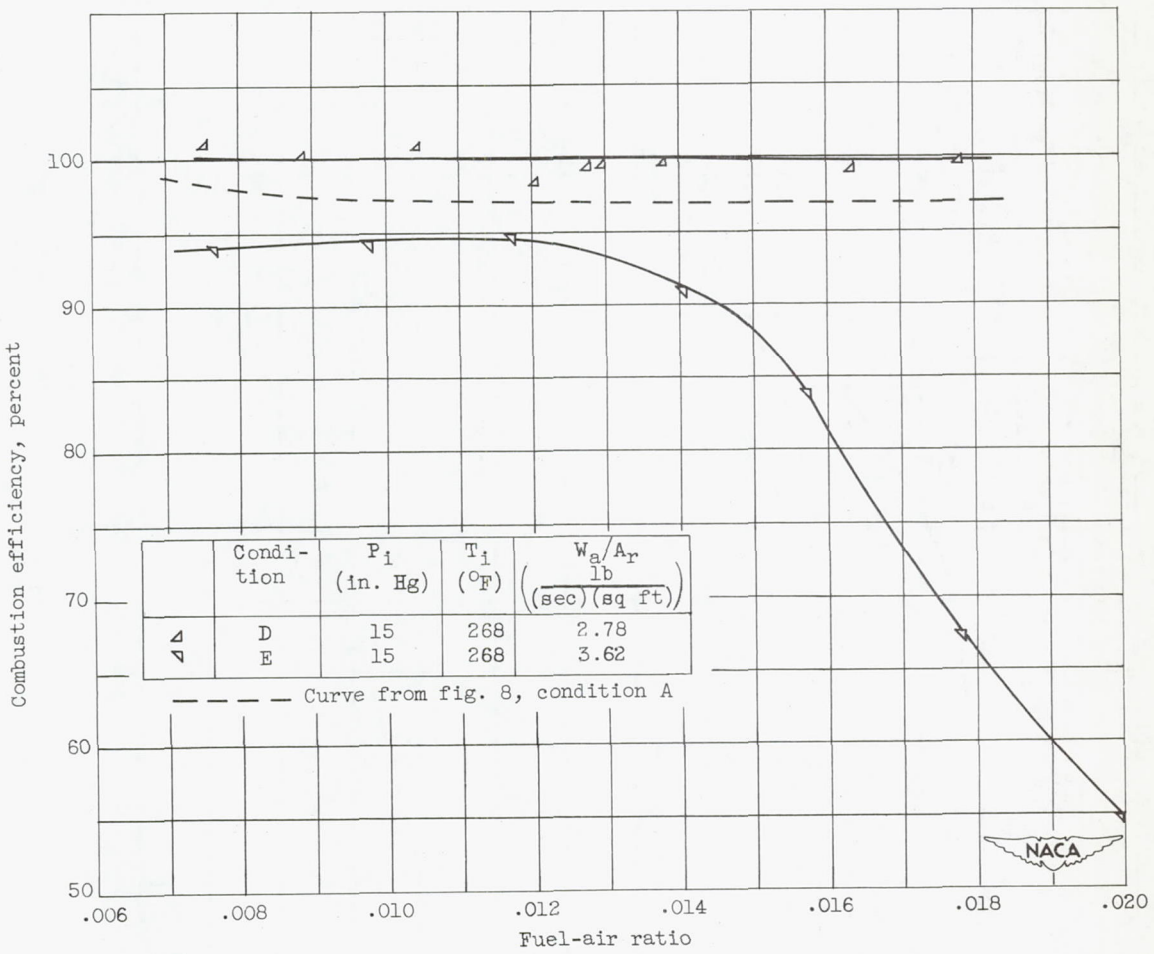


Figure 12. - Combustion efficiency of model 13 combustor with liquid MIL-F-5624A grade JP-4 fuel at various air-flow rates. 10.5-gallon-per-hour, 60° fuel atomizers.

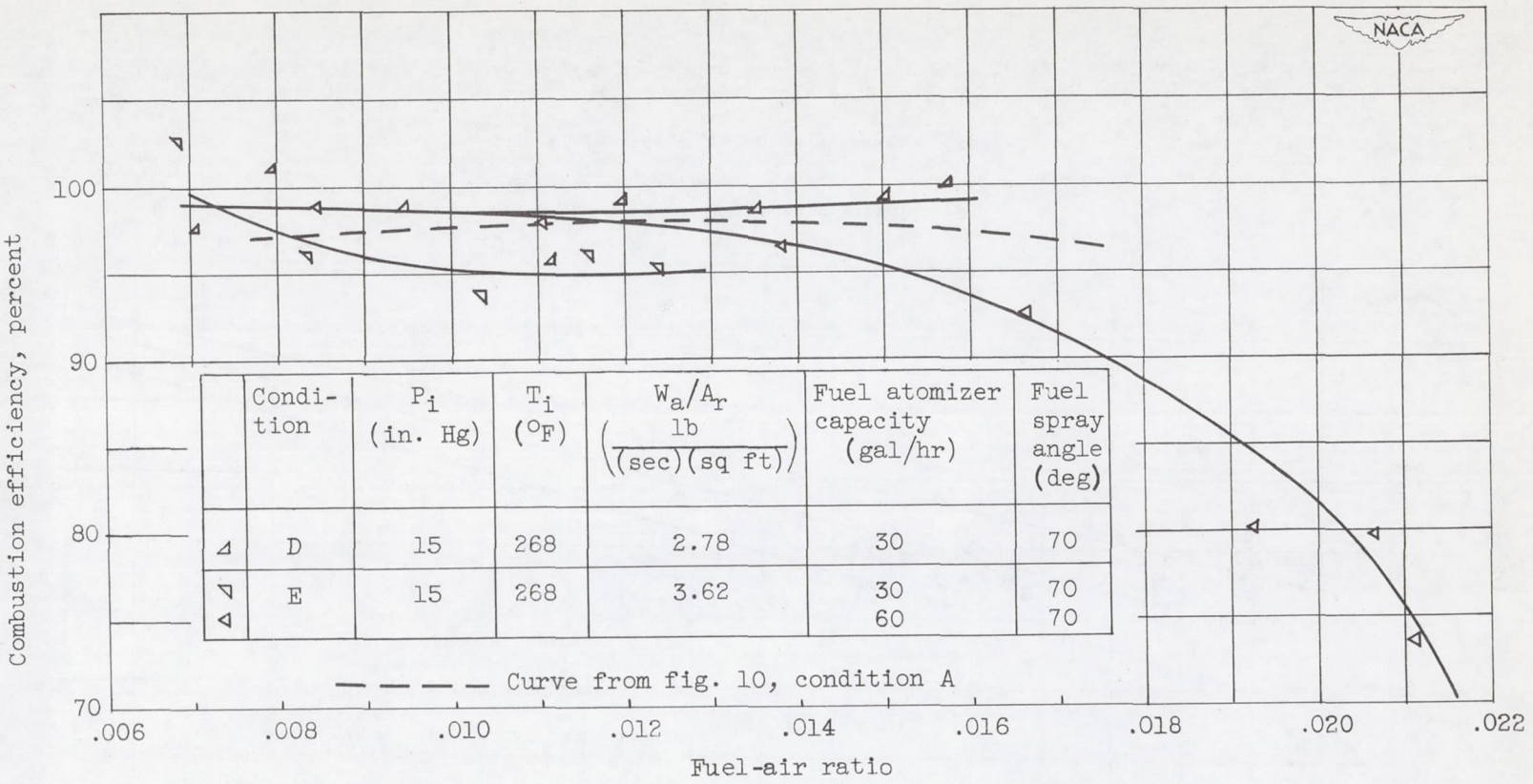


| | Condition | $P_i$ (in. Hg) | $T_i$ (°F) | $W_a/A_r$ $\left(\frac{\text{lb}}{(\text{sec})(\text{sq ft})}\right)$ | Fuel atomizer capacity (gal/hr) | Fuel spray angle (deg) |
|---|---|---|---|---|---|---|
| △ | D | 15 | 268 | 2.78 | 30 | 70 |
| △ | E | 15 | 268 | 3.62 | 30 | 70 |
| △ | | | | | 60 | 70 |

Figure 13. - Combustion efficiency of model 13 combustor with vapor (propane) fuel at various airflow rates. Two fuel atomizer capacities.

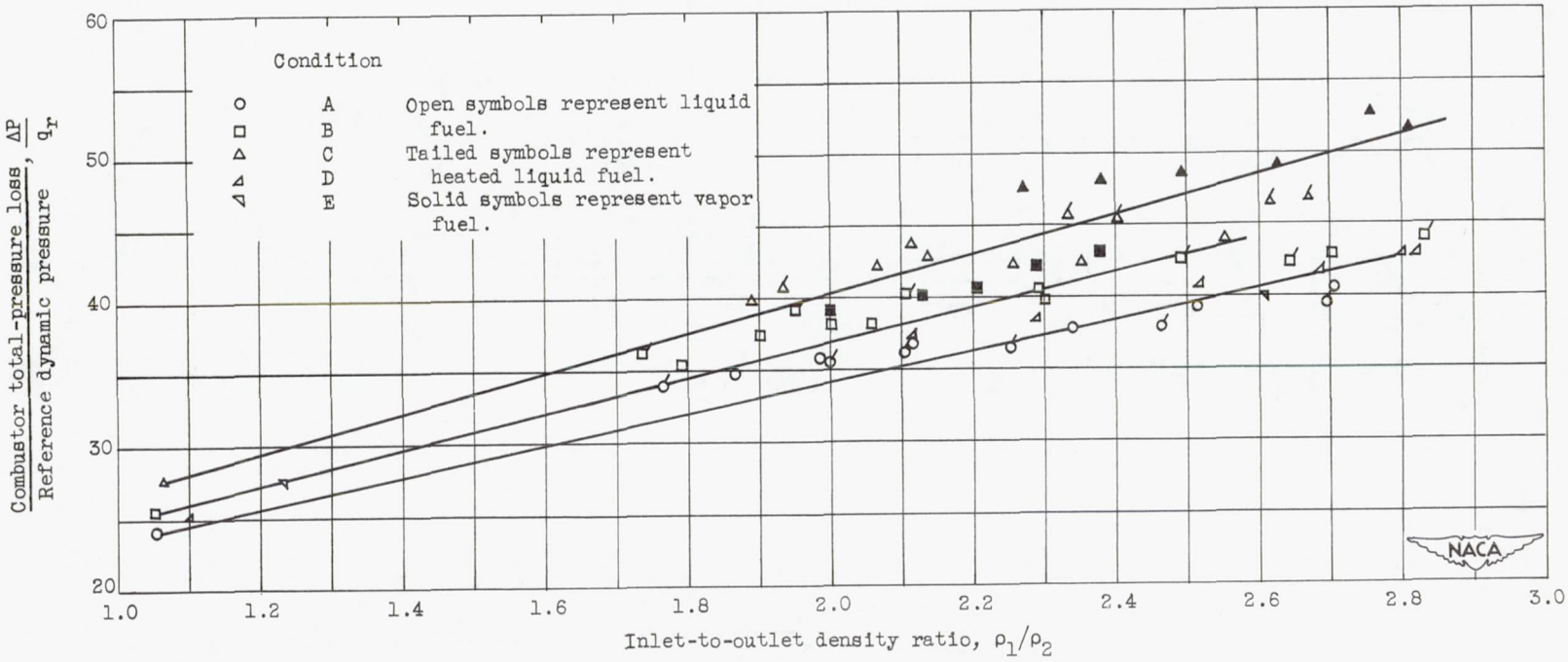


Figure 14. - Combustor pressure losses.

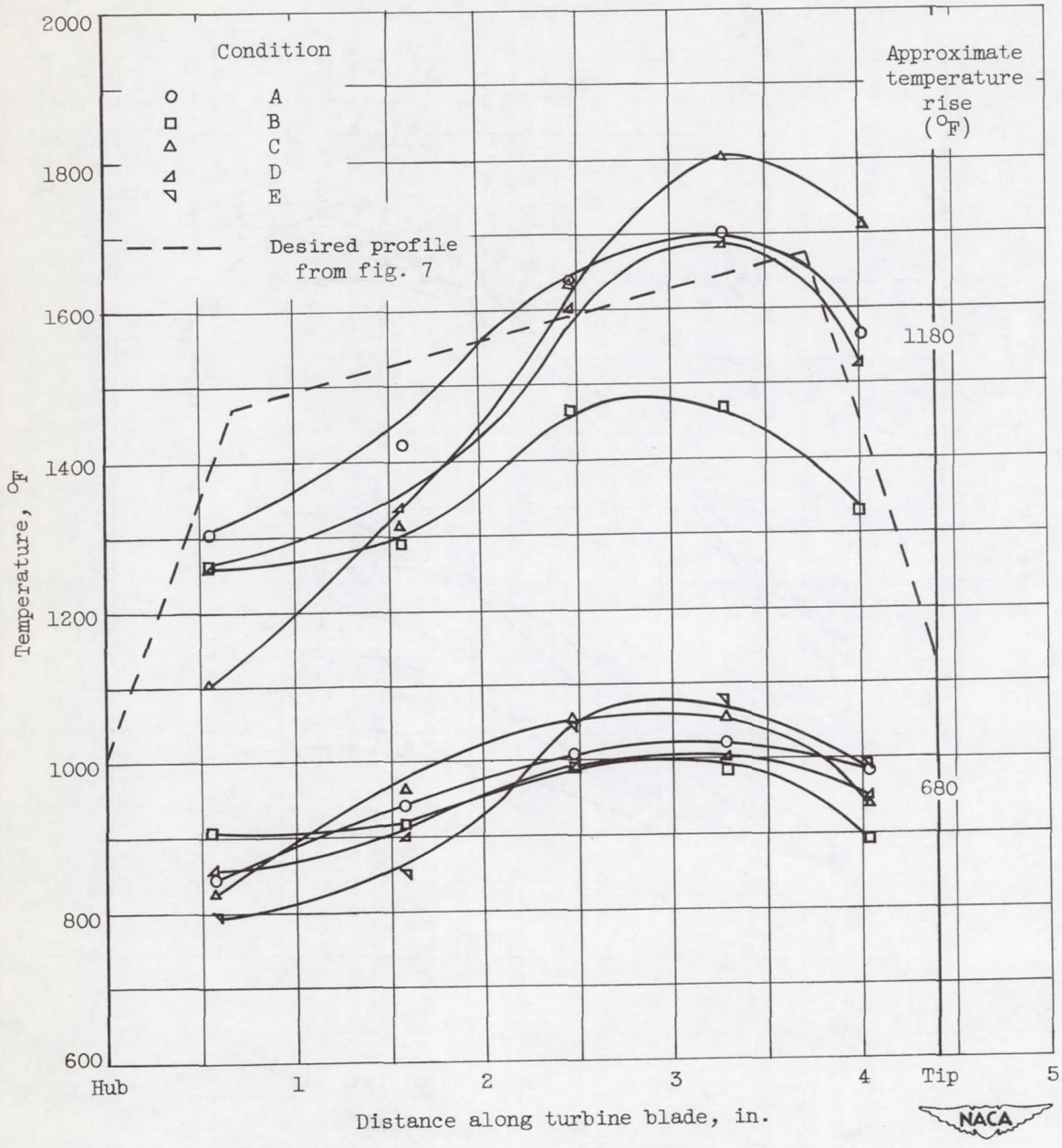


(a) Liquid MIL-F-5624A grade JP-4 fuel.

Figure 15. - Combustor-outlet temperature profiles.

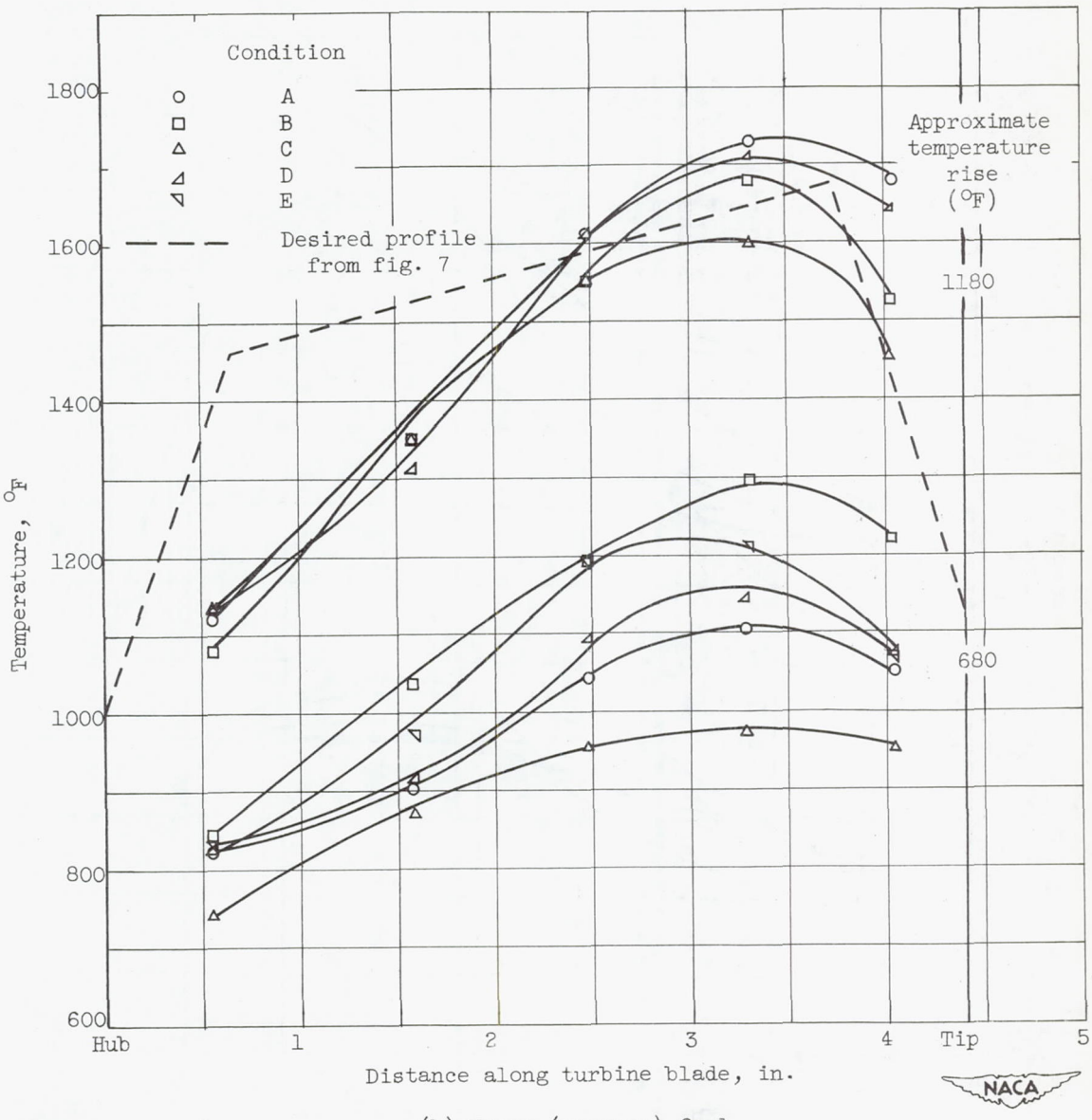


(b) Vapor (propane) fuel.

Figure 15. - Concluded. Combustor-outlet temperature profiles.

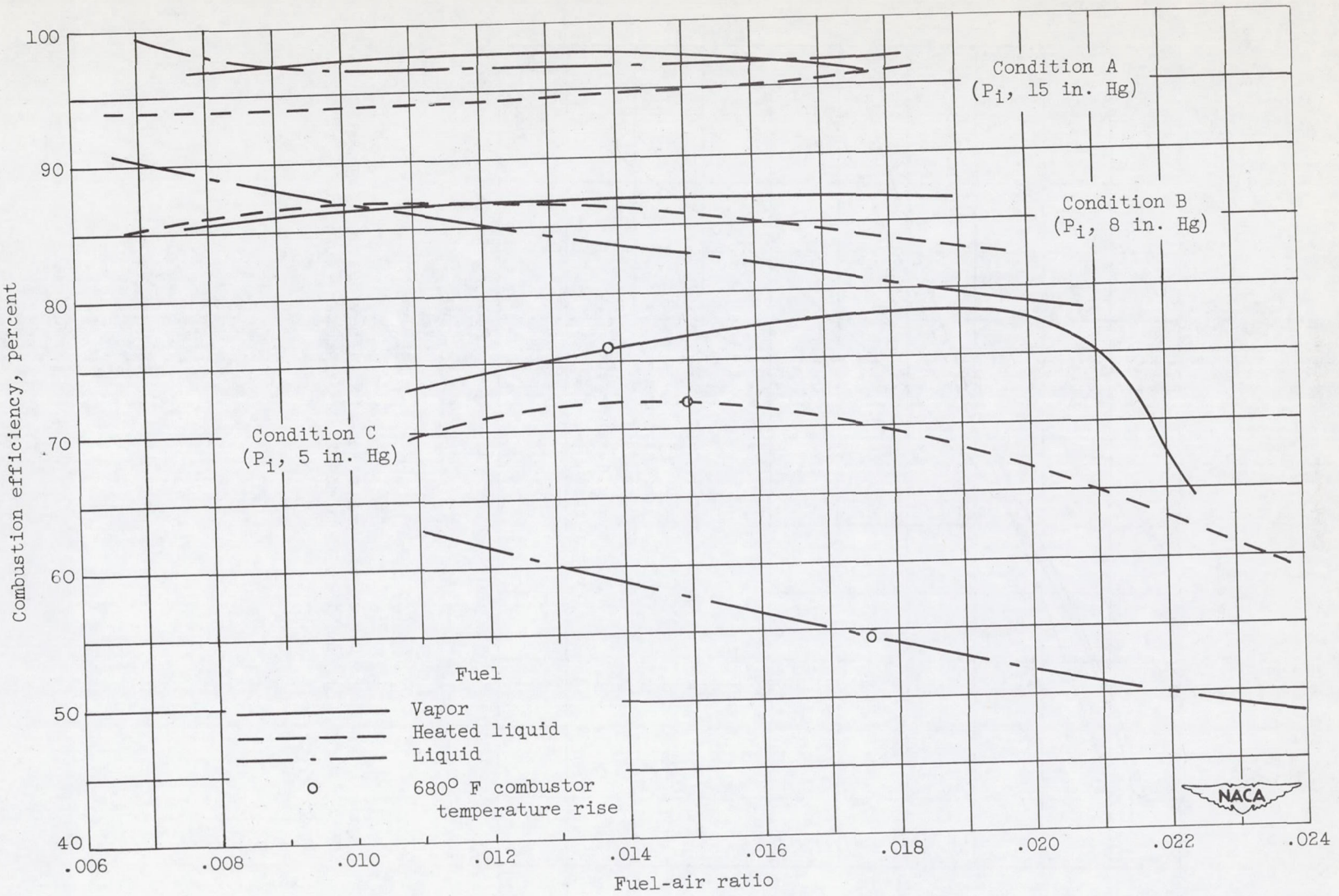


Figure 16. - Comparison of combustion efficiency for three fuel states at various pressures.

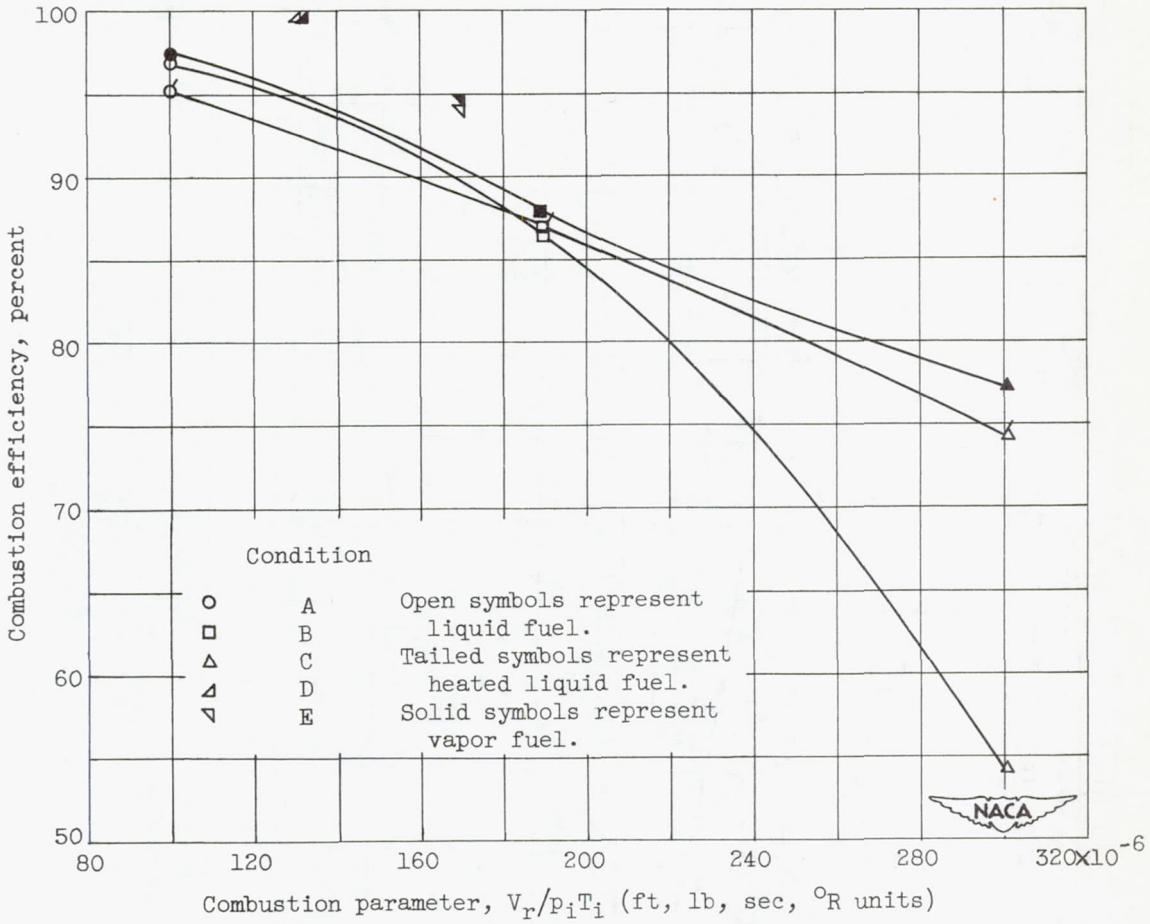


(a) Temperature rise, 680° F.

Figure 17. - Correlation of combustion efficiency data of figures 8, 9, 10, 12, and 13 with combustion parameter $V_r/p_iT_i$.

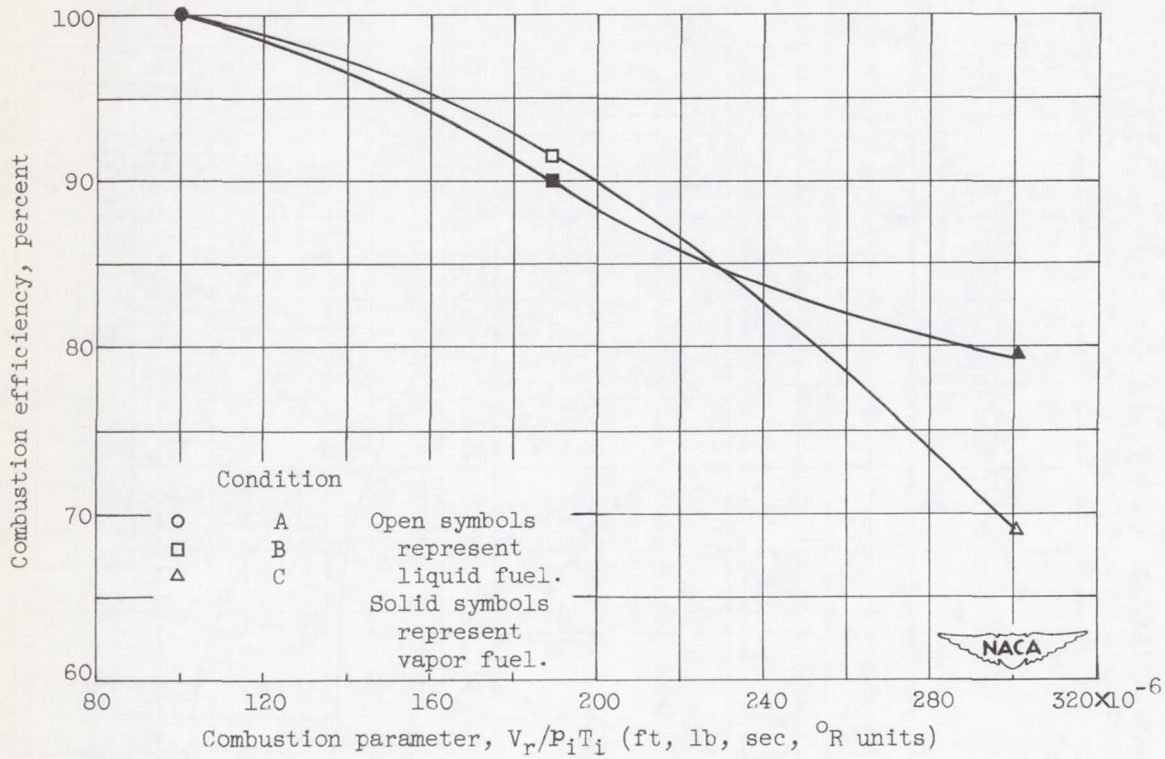


(b) Temperature rise, 402° F.

Figure 17. - Continued. Correlation of combustion efficiency data of figures 10, 12, and 13 with combustion parameter $V_r/P_iT_i$.

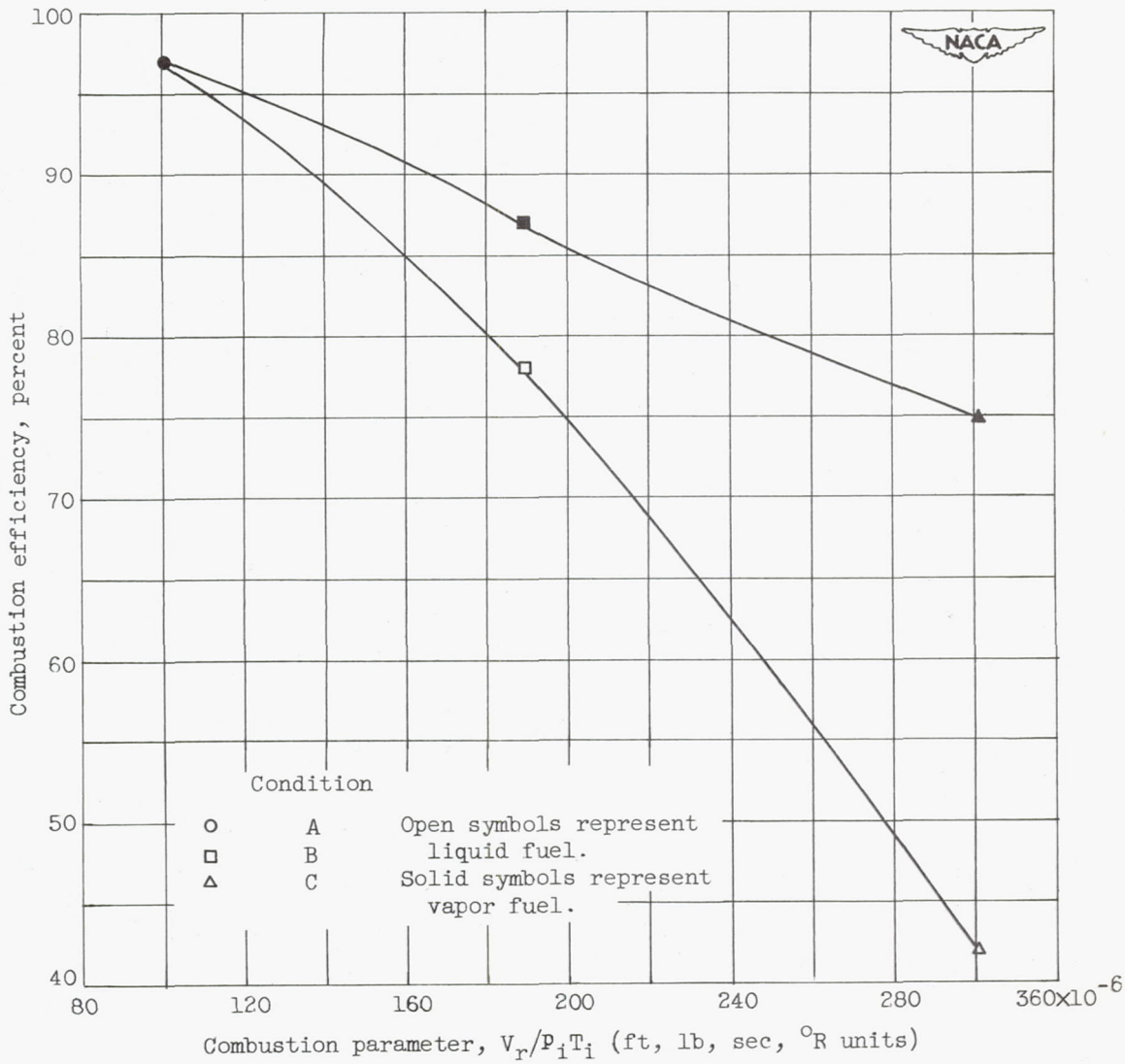


(c) Temperature rise, 1180° F.

Figure 17. - Concluded. Correlation of combustion efficiency data of figures 10, 12, and 13 with combustion parameter $V_r/P_iT_i$.

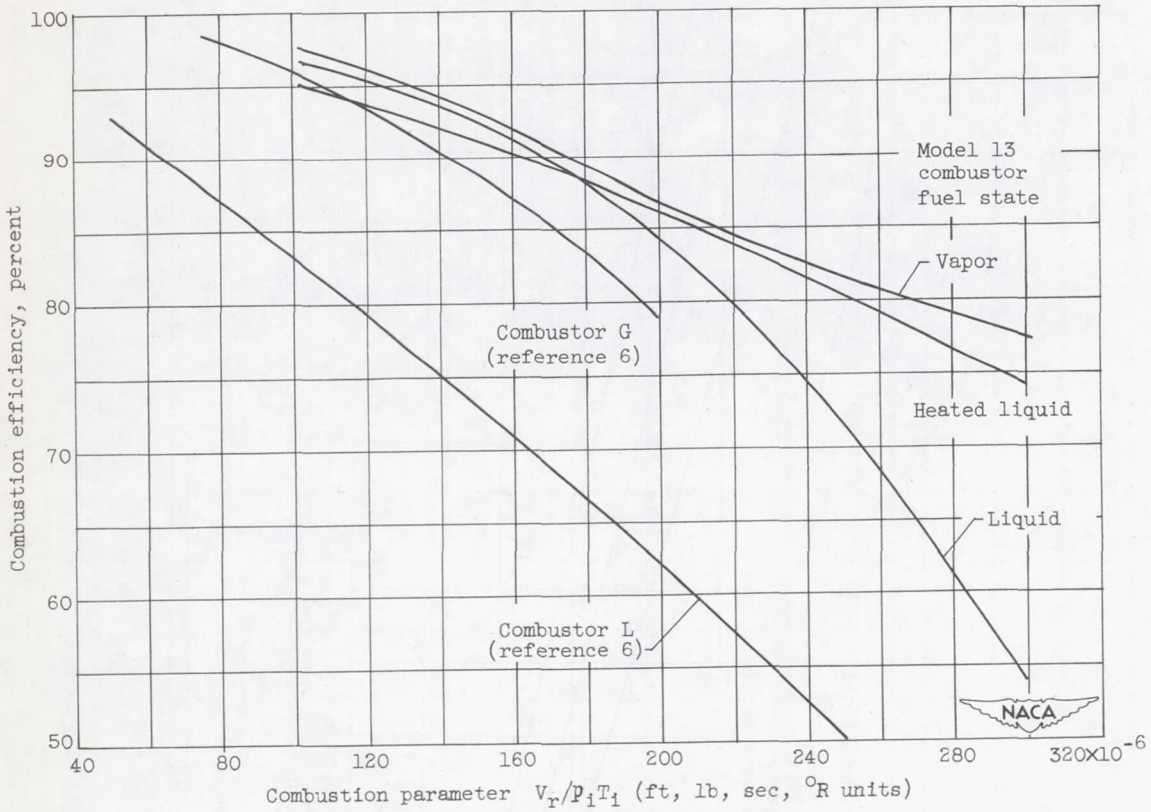


Figure 18. - Comparison of curves of figure 17 with similar curves for better combustors of reference 6.

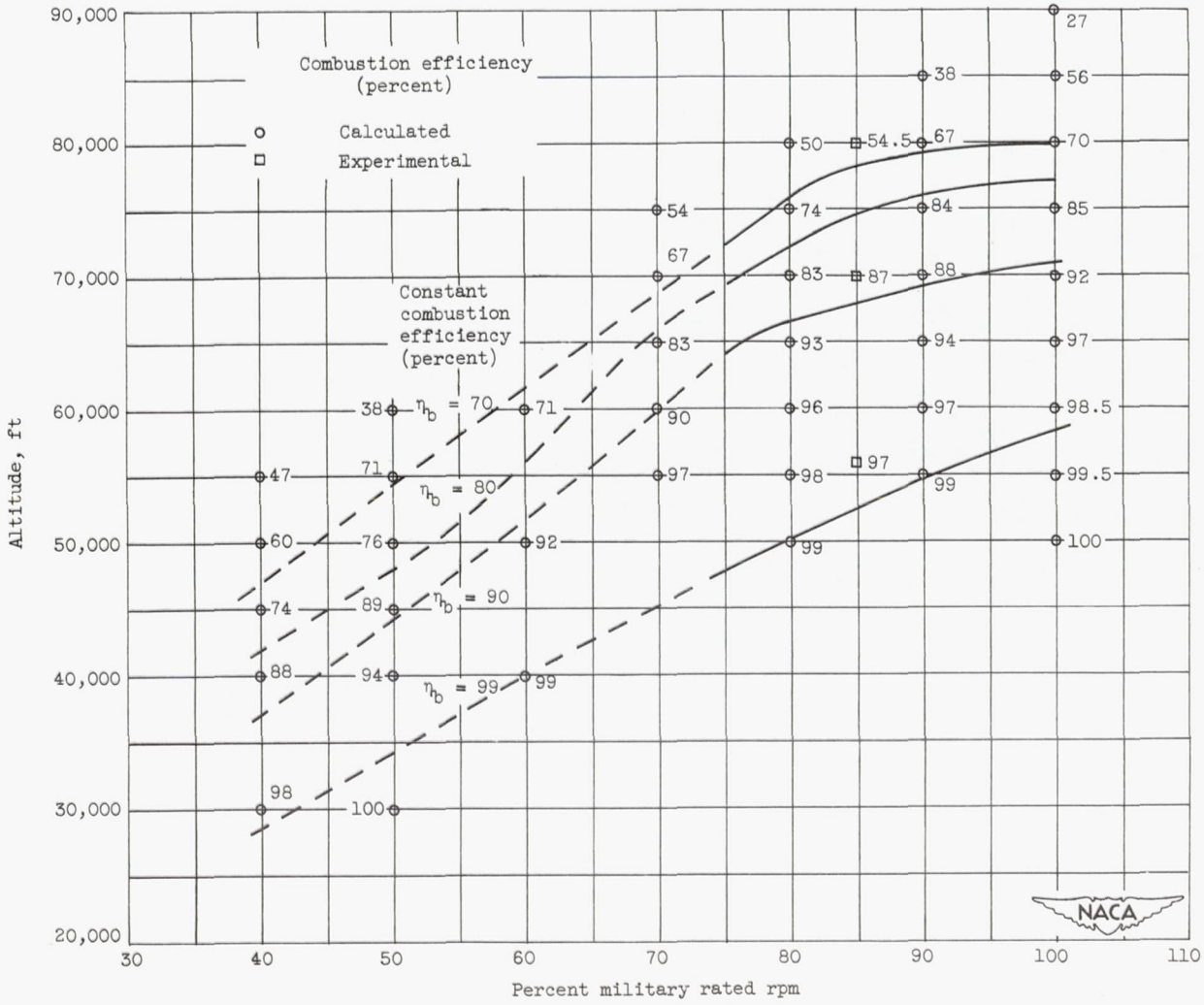


(a) Liquid MIL-F-5624A grade JP-4 fuel.

Figure 19. - Estimated altitude flight performance of model 13 combustor in 5.2 pressure ratio engine at flight Mach number 0.6.

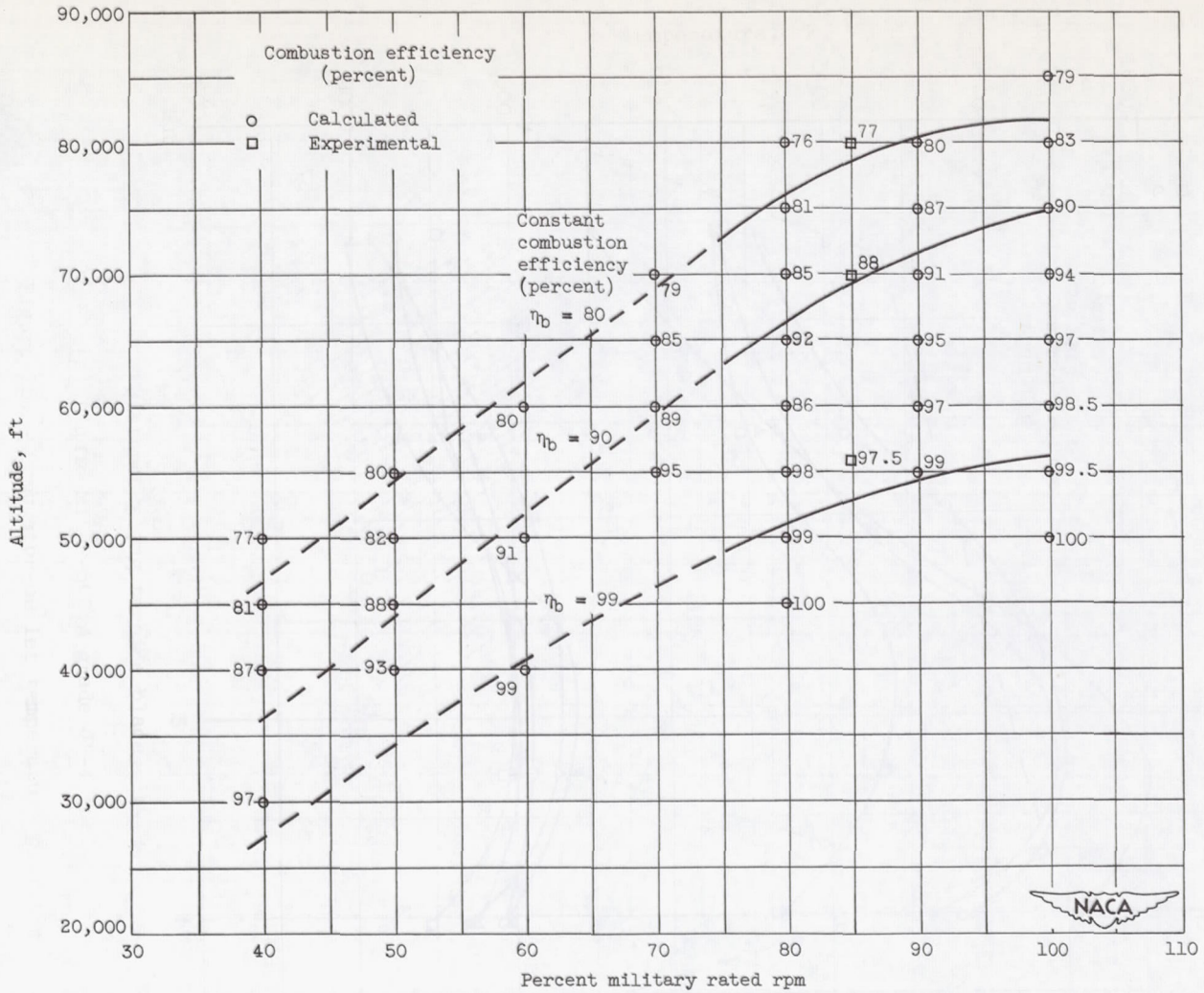


(b) Vapor (propane) fuel.

Figure 19. - Concluded. Estimated altitude flight performance of model 13 combustor in 5.2 pressure ratio engine at flight Mach number 0.6.

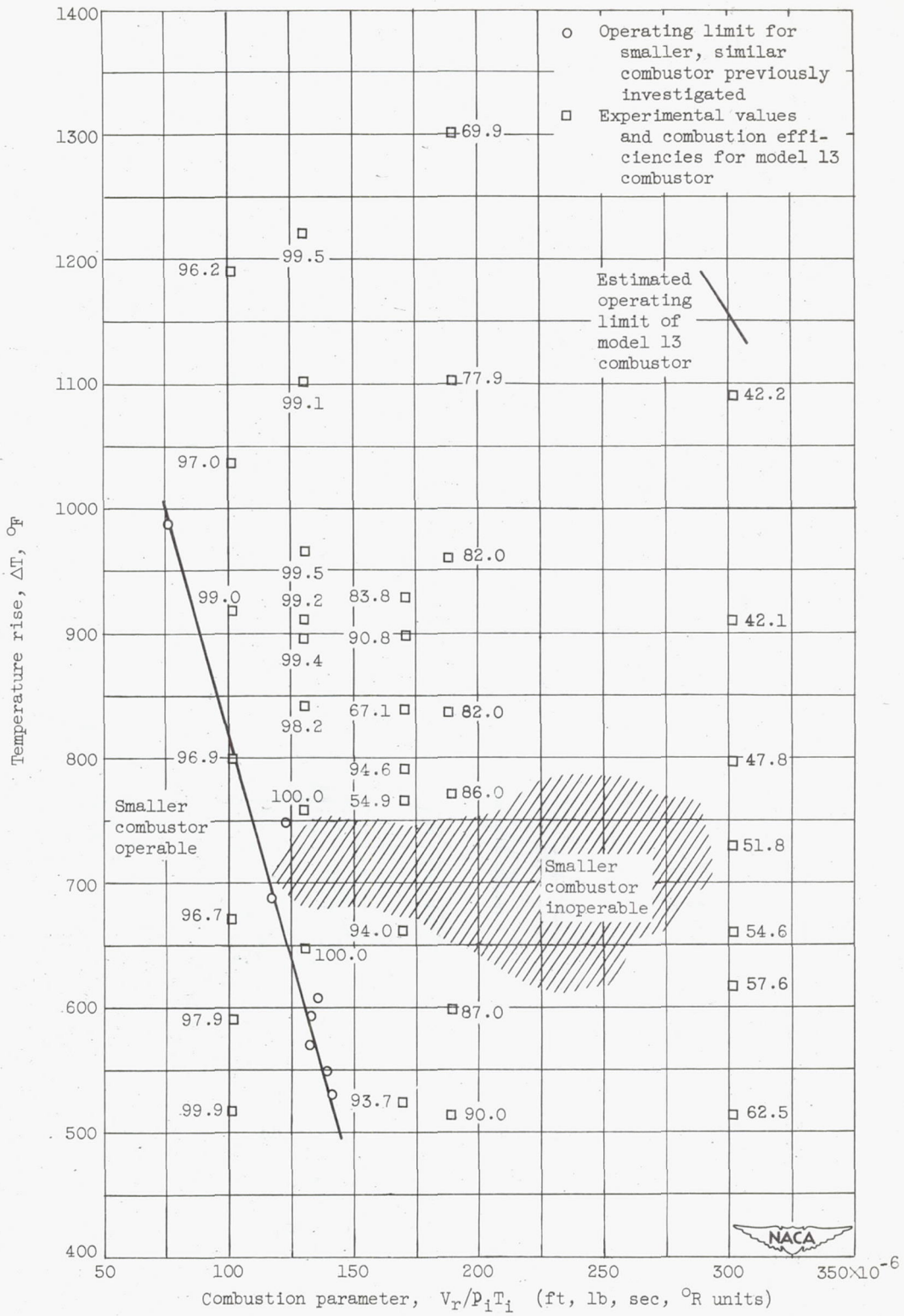


Figure 20. - Comparison of altitude performance of model 13 combustor with performance of similar combustor of smaller size.

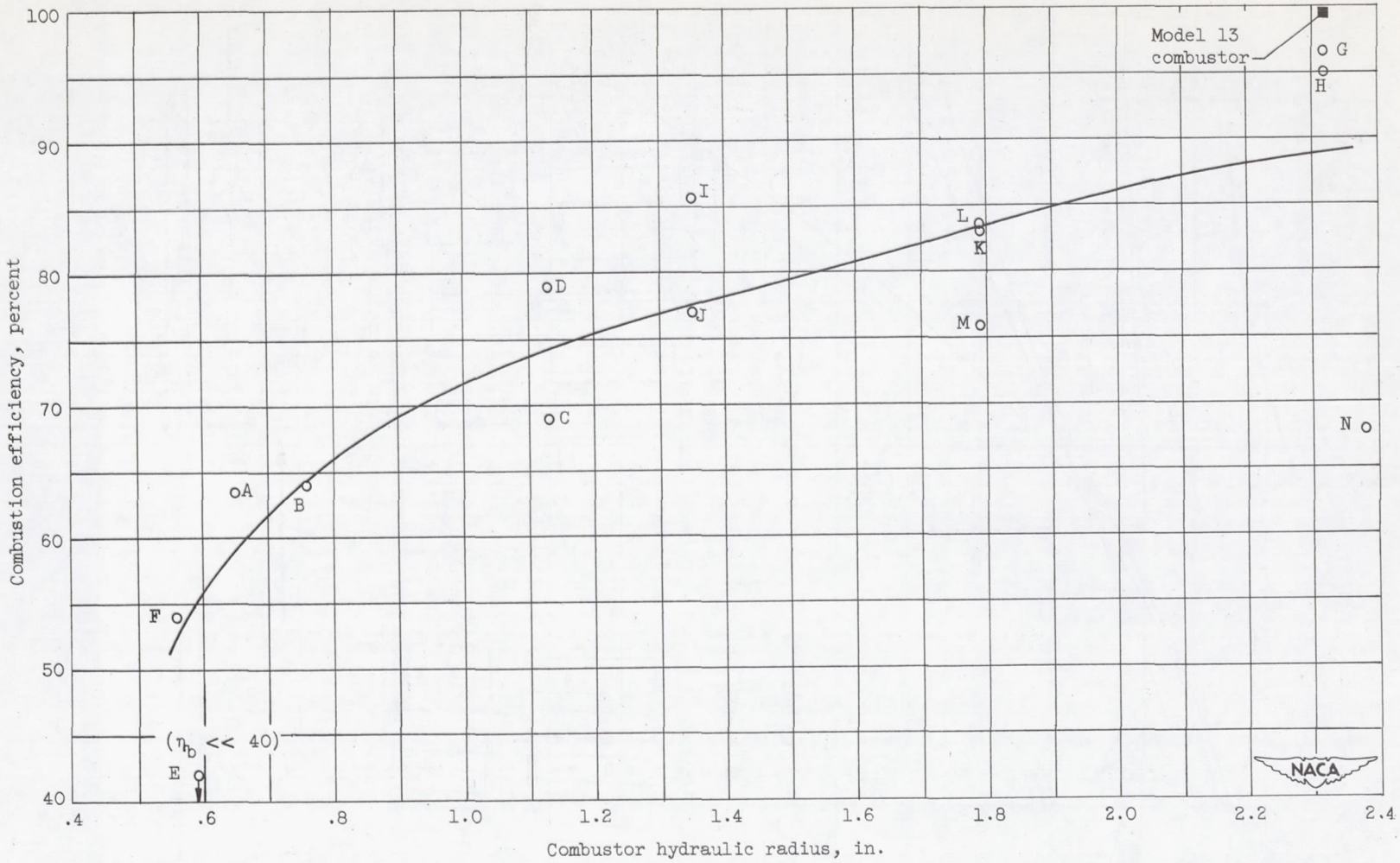


Figure 21. - Variation of combustion efficiency with combustor size at operating conditions of equal severity ($V_r/P_iT_i = 100\times10^{-6}$). Letters designate various combustors of reference 6.

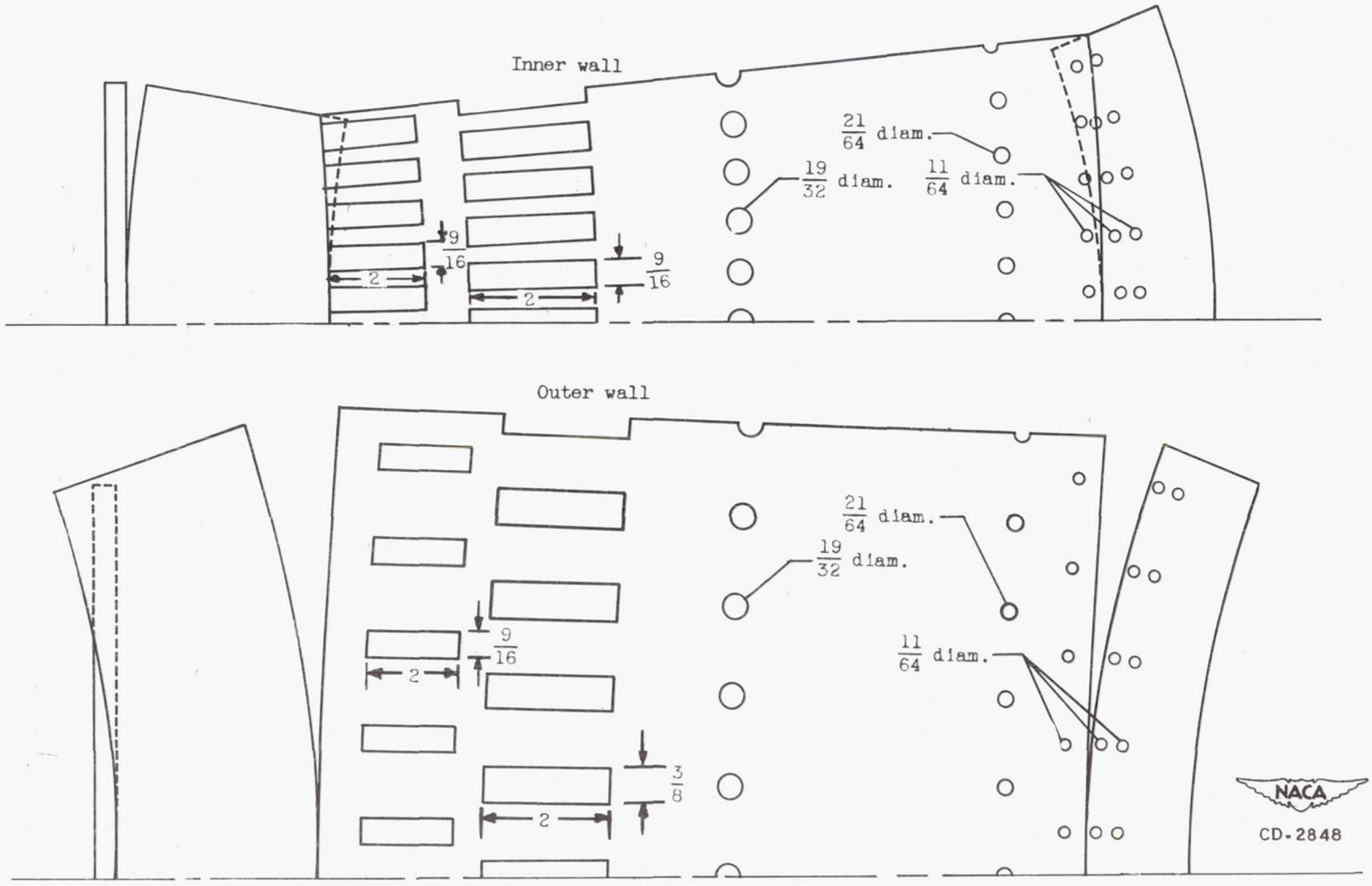


(a) Model 1.

Figure 22. - Developed view of combustor liner design for three models. (Dimensions are in inches.)

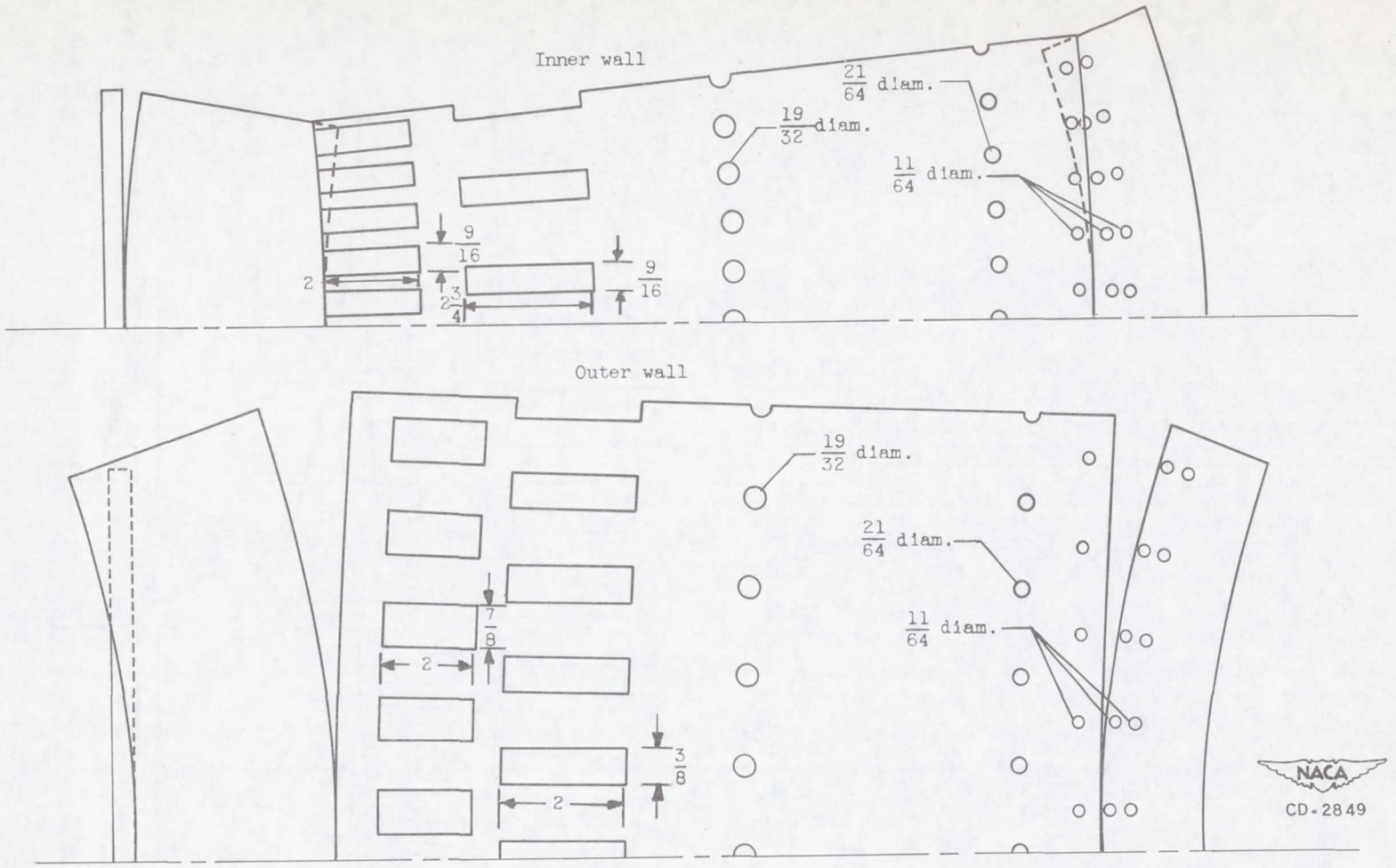


(b) Model 2.

Figure 22. - Continued. Developed view of combustor liner design for three models. (Dimensions are in inches.)

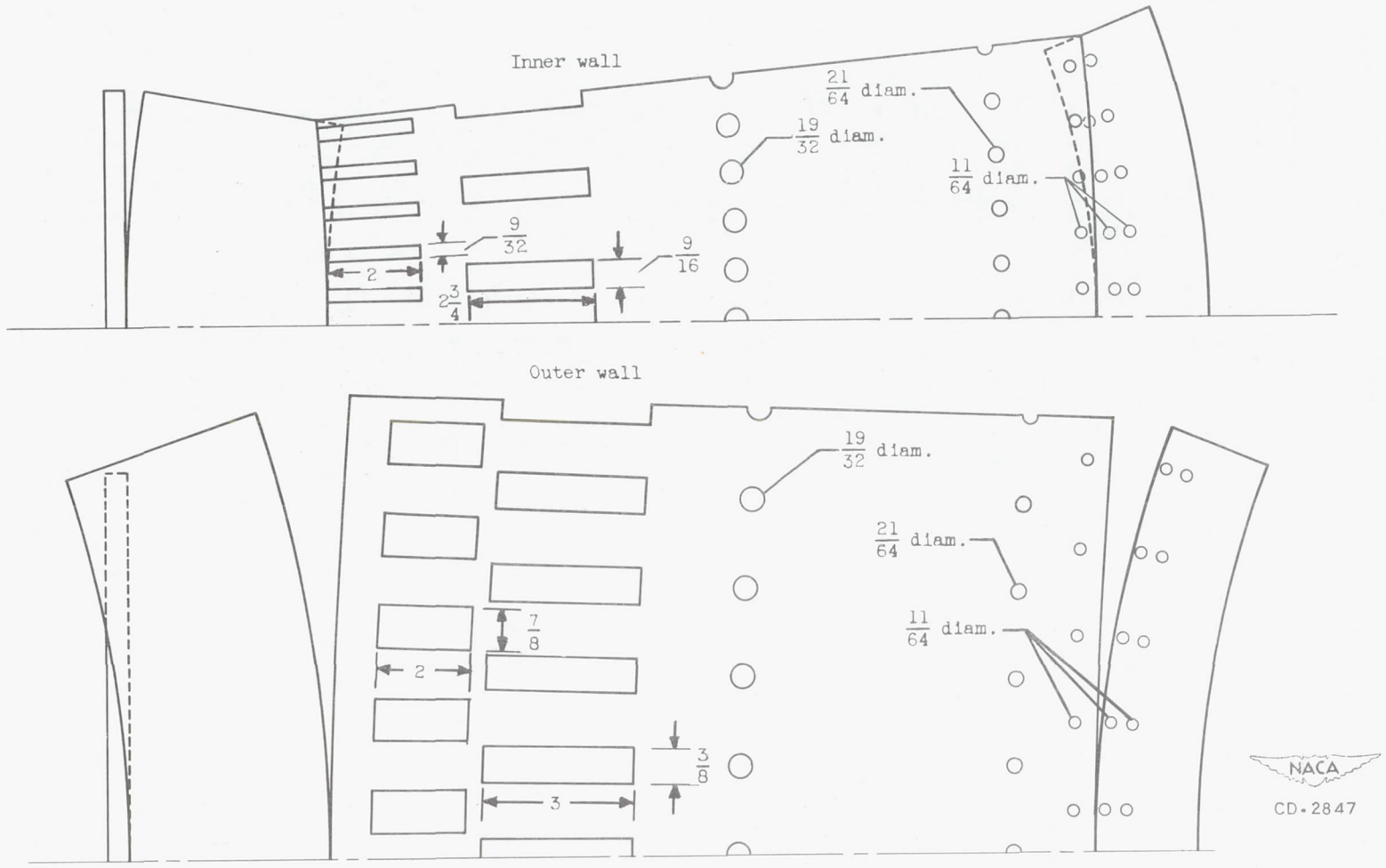


(c) Model 3.

Figure 22. - Concluded. Developed view of combustor liner design for three models. (Dimensions are in inches.)

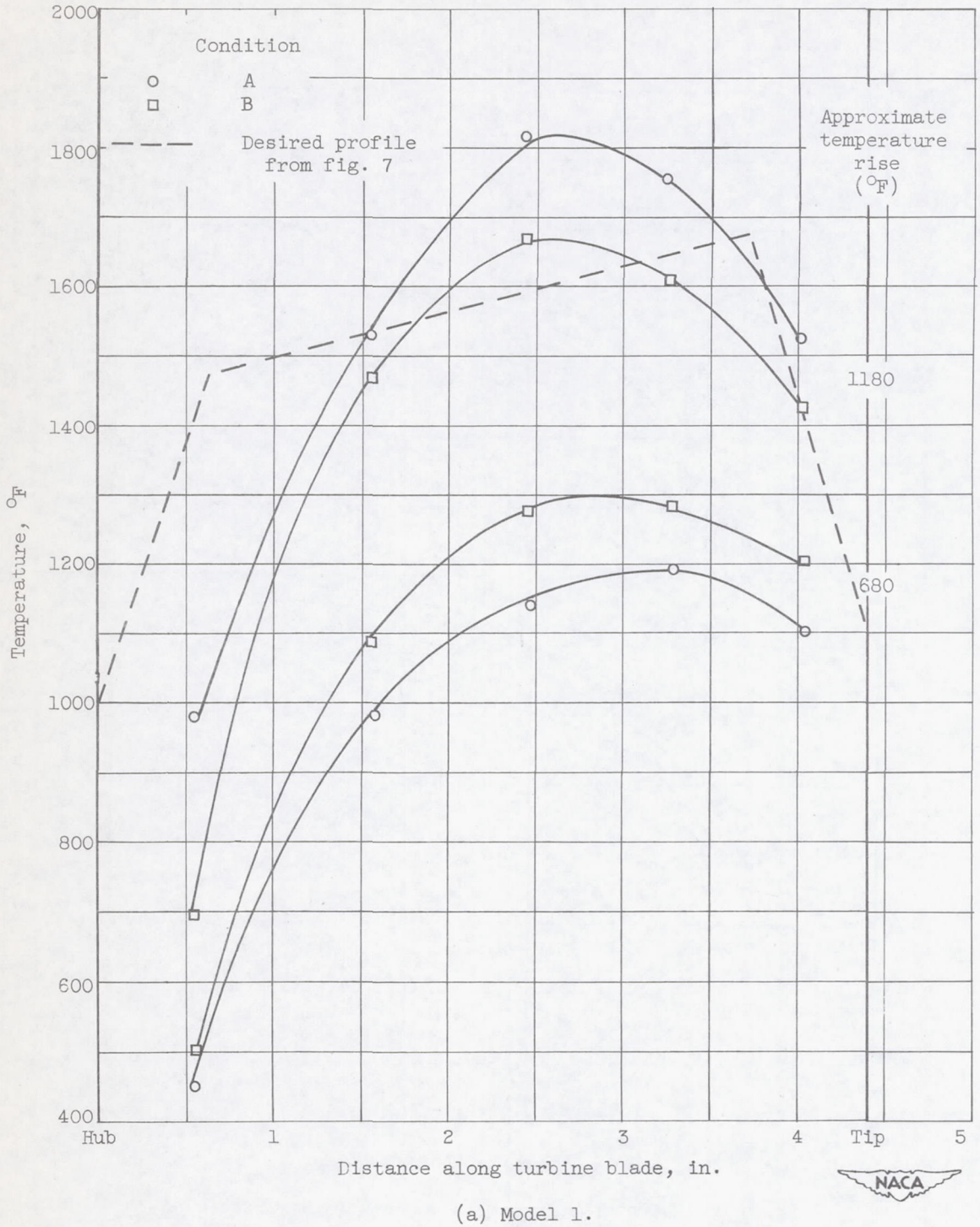


(a) Model 1.

Figure 23. - Combustor-outlet temperature profiles.

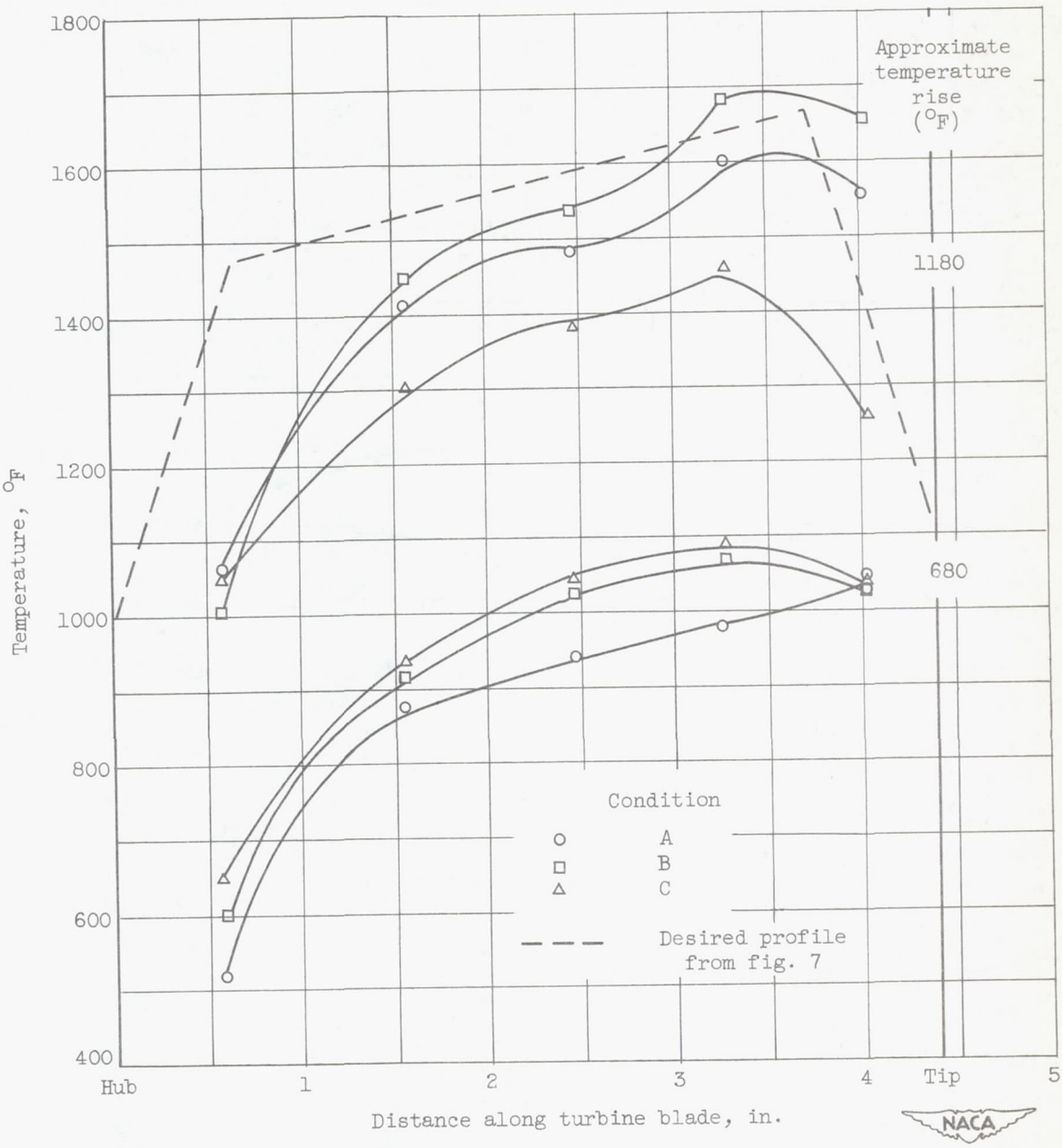


(b) Model 2.

Figure 23. - Continued. Combustor-outlet temperature profiles.

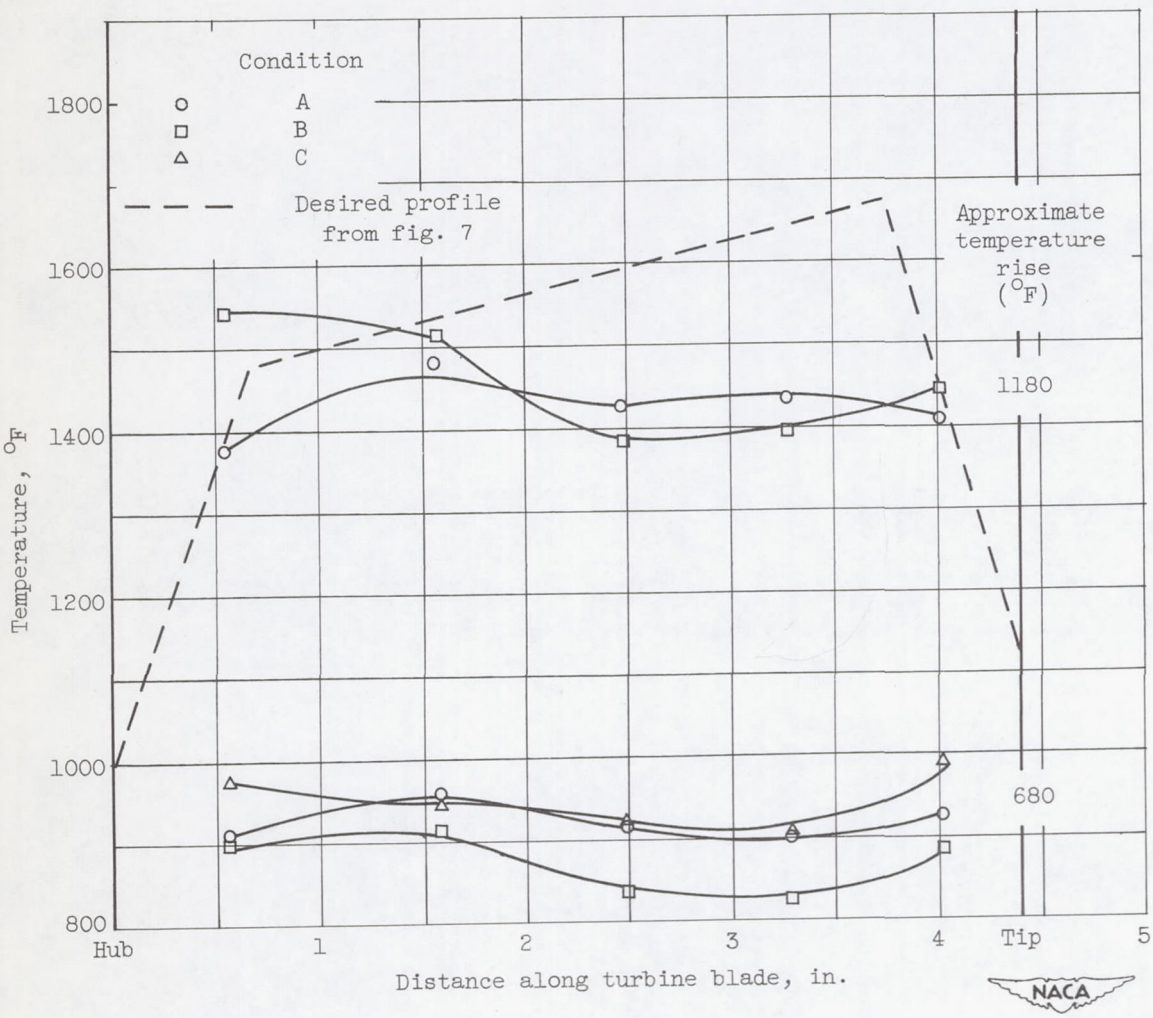


(c) Model 3.

Figure 23. - Concluded. Combustor-outlet temperature profiles.